Extracting Line Features with Wide Information in Biometrics

Yibo Zhang

A Thesis

in

Concordia Institute

for

Information Systems Engineering

Presented in Partial Fulfillment of the Requirements
for the Degree of Master of Applied Science (Information Systems Security) at
Concordia University
Montreal, Quebec, Canada

August 2007

Your file Votre référence
ISBN: 978-0-494-34789-8
Our file Notre référence
ISBN: 978-0-494-34789-8

ABSTRACT

Extracting Line Features with Wide Information in Biometrics

Yibo Zhang

Biometrics refers to the automatic identification of a person based on his/her physiological or behavioral characteristics. A biometric system is essentially a pattern recognition system which recognizes a user by determining the authenticity of a specific characteristic possessed by the user. Extracting unique features from the human body is an important task. Curvilinear structure is one of the most popular features used in biometric systems. However, even though current techniques exist to extract line features, none retain its wide information well, which is necessary in biometrics. In this thesis we propose an approach to solve this problem. After analyzing the cross-sections of given lines, we notice they are Gaussian shaped. Hence, a Gaussian filter to match them is suitable to be used. Applying a single scale filter generates a lot of noise and/or loses details. To overcome this deficiency we develop a multi-scale approach, i.e., three scales according to the cross-section widths (largest, smallest and average) as well as eight directions (horizontal, vertical and diagonal). A response is calculated by convoluting the original image with the filter. Two responses using different scales and directions form a production which exhibits less noise than a single scale filter and also preserves wide information. Two

biometric applications are applied to illustrate the effectiveness of our approach, one is for personal authentication using palm veins and another for recognizing Diabetic Retinopathy (DR) in retinal blood vessels.

Acknowledgements

During my time at Concordia University, I received an incredible amount of support and encouragement, both moral and technical, from numerous professors, researches, family and friends.

Firstly, I would like to express my gratitude and appreciation to my supervisor, Dr. Prabir Bhattacharya, for his endlessly guidance throughout my research and coursework studies. My master's degree would not have been completed without his encouragement, help, and good advice. His immense enthusiasm for research is extremely motivating.

Secondly, I would like to thank Dr. Jane You for her help and support and allowing me to join her biometric research group in Hong Kong Polytechnic University. I am also grateful to my graduate colleagues at Concordia in particular, Abu Sayeed Md. Sohail, Emad Attari, Lilybert Machacha, Mahdi Yektaii, and Kaushik Roy. They have all helped in various ways.

Last but not least I would like to thank my parents for their endless love and support.

Dedicated

To My Parents

Table of Contents

List of Figures

List of Table

Chapter 1

Overview

1.1. Why Biometrics?

Nowadays, the question of identity is asked numerous times a day. We are required to identify ourselves for almost everything we do as the need for security increases. Questions such as "Does the person have access to these files?", "Is the person authorized to perform this transaction?" and others alike are asked millions of times a day. All these relate back to the primary question of identity [1-11].

As of now there are two common ways of solving this question, one is what you know and the other is what you have. What you know refers to passwords or PIN which can be entered into systems that grant you access and authorization. This is not convenient since we have to remember so many. What you have on the other hand refers to physical keys, like ID cards. Physical keys can also be stolen, lost or even forged with devastating consequences. These two traditional solutions are not ideal and their problems have led governments and businesses to lose millions of dollars due to illegal access and security breaches [10].

The question is now, "Is there another way to solve the problem of identity?". Currently the best solution is biometrics. Biometrics refers to the automatic

authentication of a person based on his/her physiological or behavioral characteristics [11].

Because biometrics is based on physiological or behavioral characteristics which are unique to every individual, it implies that the technique used is nearly foolproof [5-11]. This is due to the fact that ones characteristics cannot be stolen, forgotten, duplicated or shared.

According to IBG (International Biometric Group), biometrics is an ever growing industry as can be seen in Fig. 1.1. For example, the total biometric industry revenues will be over 3 billion this year and up to 7.4 billion in 2012. The market share of different biometrics in 2007 can be shown in Fig. 1.2.

1.2. What is Biometrics?

Definitions

The term biometrics, strictly speaking, refers to a science involving the statistical analysis of biological characteristics. For a physiological or behavioral attribute to be considered a suitable biometric it must have the following properties [2-5]:

- *Universality*, which indicates that every person should have the characteristic;

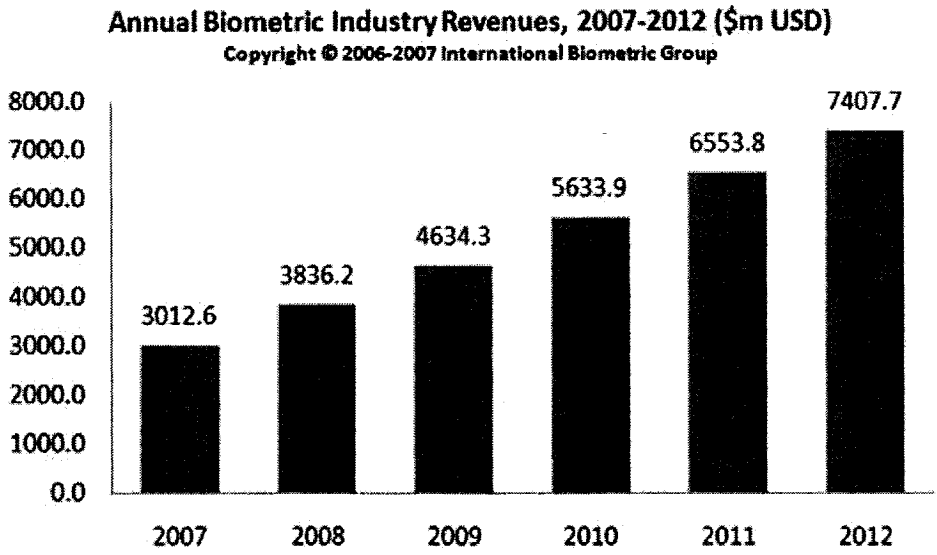

Figure 1.1 Annual biometric industry revenues, 2007-2012 ($m USD).

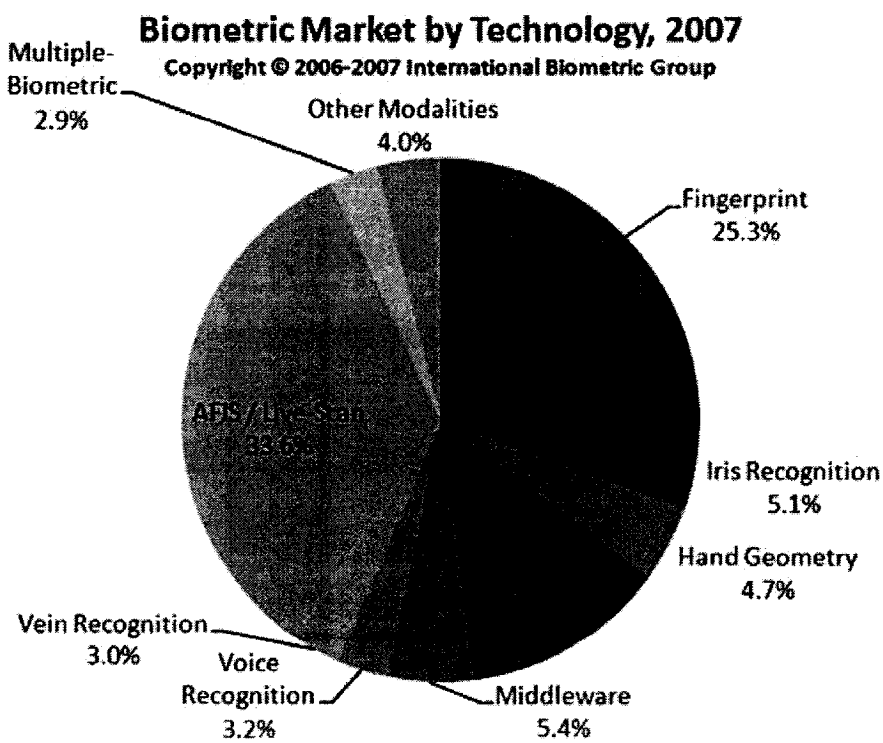

Figure 1.2 Biometric market by Technology, 2007.

- *Uniqueness*, which means that any two persons should be different enough to distinguish each other based on this characteristic;
- *Permanence*, which indicates that the characteristic should be stable enough and not change significantly with environment or time;
- *Collectability*, which means that the characteristic can be measured quantitatively;
- *Acceptability*, which indicates to what extent people are willing to accept the biometrics system;
- *Performance*, which refers to the achievable identification accuracy, the resource requirements to achieve an acceptable identification accuracy and the working or environment factors that affect the identification accuracy;
- *Circumvention*, which refers to how easy it is to fool the system by fraudulent techniques.

The following are physiological and behavioral features that satisfy the above properties [6-11].

Physiological characteristics:

— Skin pores;

— Wrist/hand veins;

— Chemical composition of body odor;

(a) Fingerprint

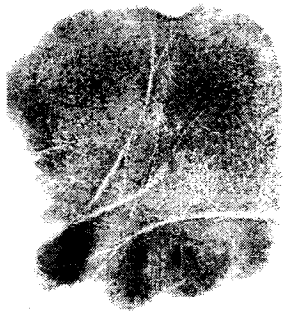

(b) Palmprint

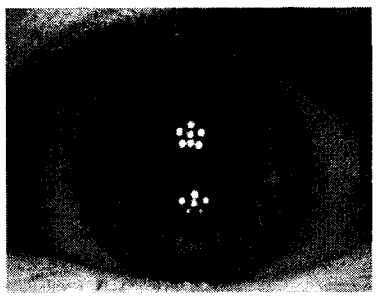

(c) Iris

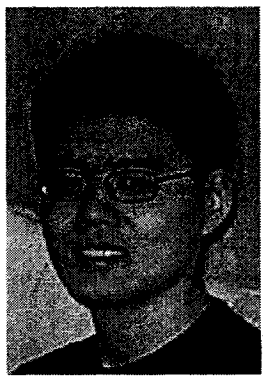

(d) Face

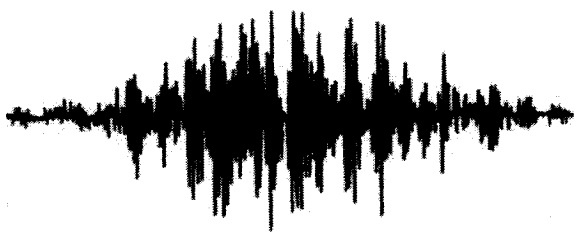

(e) Voiceprint

(f)Handwriting signature

Figure 1.3 Typical physical characteristics: (a) Fingerprint; (b) Palmprint; (c) Iris and (d) Face, and Behavioral characteristics: (e) Voiceprint and (f) Handwriting signature.

— Palm-prints;

— Facial features and thermal emissions;

— Hand geometry;

— Features of the eye, i.e., retina and iris;

— Fingerprints.

Behavioral characteristics:

— Gait;

— Handwritten signature;

— Gesture;

— Voiceprint;

— Keystrokes or typing.

Widely used physiological and behavioral biometrics are explained below with some illustrated in Fig. 1.3.

Face

Face recognition is a non-intrusive method while facial images are probably the most common biometric characteristic used by humans to recognize each other. The applications of facial recognition ranges from a static controlled mug-shot to a dynamic uncontrolled facial identification in a busy street. The most popular

approaches to face recognition [12] are based on either (i) the location and shape of facial attributes, such as the eyes, eyebrows, nose, lips and chin and their spatial relationships or (ii) the overall (global) analysis of the face image that represents a face as a weighted combination of a number of canonical faces. The advantages of face recognition are cheap hardware components and the ability to operate without user cooperation. Its disadvantages include, changes in both acquisition environment and physiological characteristics reduce matching accuracy, i.e. outdoor instead of indoor and it cannot handle identical twins.

Fingerprint

Humans have used fingerprints for personal identification for many centuries [13] and the matching accuracy using fingerprints has been shown to be very high [14]. A fingerprint is the pattern of ridges and valleys on the surface of a fingertip [15-16]. Fingerprints of identical twins are different and so are the prints on each finger of the same person. One problem with the current fingerprint recognition system is that they require a large amount of computational resources especially when operating in the identification mode. Also, fingerprints from a small fraction of the population may be unsuitable for automatic identification because of genetic factors, aging, environmental or occupational reasons (e.g., manual labor workers may have a large

number of cuts and bruises on their fingerprints).

Hand Geometry

Hand geometry recognition systems are based on a number of measurements taken from the human hand, including its shape, size of palm, lengths and widths of the fingers. Commercial hand geometry-based verification systems have been installed in hundreds of locations around the world [3][101]. The technique is very simple and inexpensive. Compared with fingerprint, hand geometry uses less storage requirement and is more acceptable. Environmental factors such as dry weather or individual anomalies such as dry skin do not appear to have any negative effects on the verification accuracy of hand geometry-based systems. However, the shape of the human hand is not guaranteed to be unique.

Iris/Retina

Both iris and retina are from the eye. The iris is the annular region of the eye bounded by the pupil and the sclera (white part of the eye) on either side [17-20]. The complex iris texture carries very distinctive information useful for personal recognition. The accuracy and speed of currently deployed iris-based recognition systems is promising [21] and point to the feasibility of large-scale identification systems based on iris

information. Each iris is distinctive and like fingerprints even the irises of identical twins are different. It is extremely difficult to surgically tamper the texture of the iris. Further, it is rather easy to detect artificial irises (e.g., designer contact lenses). Although, the early iris-based recognition systems required considerable user participation and were expensive, the newer systems have become more user-friendly and cost-effective.

As a member of the biometric family, retina provides the highest accuracy compared to other family members [19-21]. This biometric system works by scanning and analyzing the layer of the blood vessels at the back of the eye (see Fig. 5.2(a)). Scanning involves using a low-intensity light source and an optical coupler to look for unique patterns in the retina [80-84]. A major disadvantage of this application is that users place their eye close to the capture device and focus on a certain point. This can cause discomfort to some as they fear their eye maybe in danger of being damaged.

Signature

The way a person signs their name is a characteristic of that individual. Signatures are a behavioral biometric that change over a period of time and are influenced by physical and emotional conditions of the signatories [22]. Signatures of some people vary substantially and even successive impressions of their signature are significantly

different. Furthermore, professional forgers may be able to reproduce signatures that fool systems [23].

Voice

Voice is a typical behavioral biometrics [24]. The features of an individual's voice are based on the shape and size of the appendages (i.e., vocal tracts, mouth, nasal cavities, and lips) that are used in the synthesis of sound. These physiological characteristics of human speech are invariant for an individual while the behavioral part of the speech changes over time due to age, medical conditions (such as common cold), emotional state, etc. Voice is also not very distinctive and may not be appropriate for large-scale identification. A disadvantage of voice-based recognition is that speech features are sensitive to a number of factors such as background noise. Speaker recognition is most appropriate in phone-based applications but the voice signal over the phone is typically degraded over the communication channel.

Palmprint

Palmprint recognition [25] is an emerging technology and is based on the inside part of a human's hand from the wrist to the end of the fingers. Automatic palmprint identification systems can be classified into two categories: on-line and off-line. There

are three key issues to be considered in developing an on-line palmprint identification system [26]: palmprint acquisition, palmprint feature representation and palmprint identification. The palm provides a larger surface area compared with fingerprint, so more features can be extracted [27]. However, since this is a new biometric technology, it still requires testing on large databases [28]. Palmprint recognition systems have the potential to be used in criminal investigation, human resources management, physical access control, access control to portable device, disease diagnosis, fortune telling, immigration and emigration control, e-commerce...etc.

1.3. Biometrics Systems

System Architecture

A biometrics system is divided into two phases, Enrollment and Identification [6]. In enrollment phase, a biometric characteristic is captured, its feature(s) extracted and stored as a template in the database. For identification the first two steps of enrollment are repeated but instead of storing the template, it is compared with every other template in the database to find a match. These two phases are shown in Fig. 1.4. The components of the phases are described below.

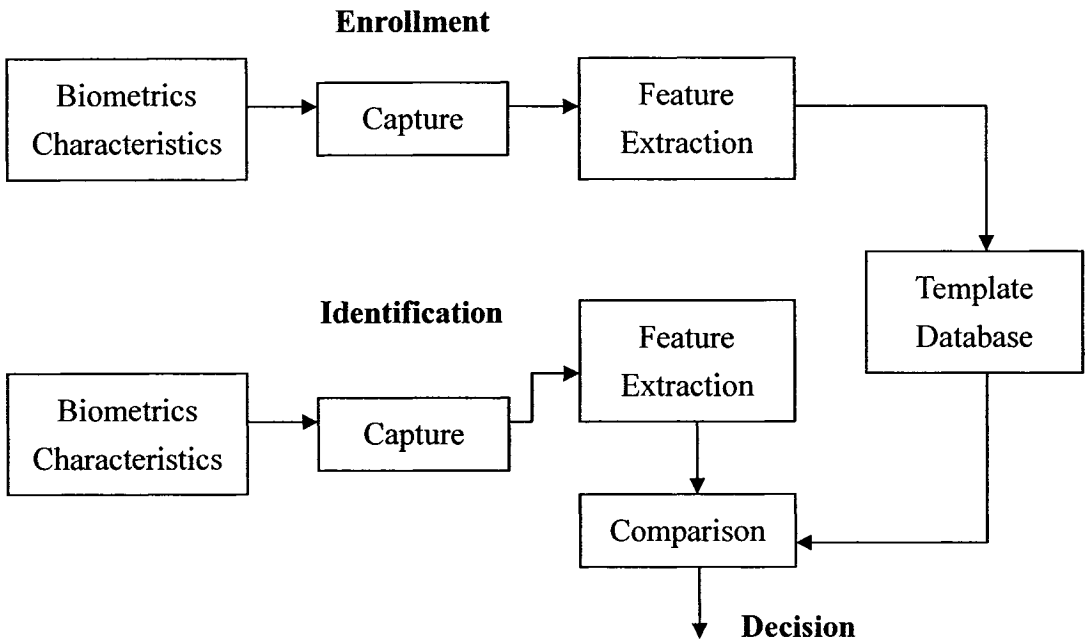

Figure 1.4 General procedure of biometrics systems.

Capture

This component consists of capturing the physiological or behavioral characteristics using different devices. Once captured, some preprocessing is performed to remove noise and enhance edge(s) in the digital image. The most common tool used here is some sort of camera.

Feature Extraction

After the characteristic is captured with noise removed and edge(s) enhanced, unique features are extracted from the image to create a template. Templates from different individuals are distinguishable while templates coming from the same person should

not diverge too much.

Comparison

The template just created in the previous component is compared with all other templates in the database. A matching score is customarily calculated here for use in the next stage.

Decision

This is the final component of the biometrics system. Here the matching score is evaluated against a predefined threshold. In the general case if the matching score is greater than or equal to the threshold the template belongs to that class and an output of 'yes' is produced. If the template is less than the threshold this signals that the template does not belong to that class and "no" is outputted.

Verification vs. Identification

An important distinction between verification and identification in biometric systems needs to be made. Verification refers to a 1-to-1 matching while Identification is 1-to-Many [29]. This means when a user first enters his/her PIN the system automatically fetches their template and compares it to a newly generated one just

scanned (1-to-1 matching). In the other case the user does not enter a PIN so the system has to compare this template just created with every other existing one in the database (1-to-Many). Fig. 1.5 gives a pictorial view of this.

Biometrics System Performance Evaluation

FAR (False Acceptance Rate) and FRR (False Rejection Rate) are two ways (Fig. 1.6) to measure the accuracy of biometrics systems [1][30-31]. FAR measures the number of false template matches accepted by the system when it shouldn't. FRR measures the number of true template matches that should be accepted by the system but are not. Both FAR and FRR can be calculated by:

$$FAR = \frac{TotalFalseAccept}{TotalFalseAttempts} \times 100\% \tag{1.1}$$

$$FRR = \frac{TotalFalseNonAccept}{TotalTrueAttempts} \times 100\% \tag{1.2}$$

The vertical line in the middle of the graph in Fig. 1.6 represents ERR (Equal Error Rate), which can be defined as:

$$FAR = FRR \tag{1.3}$$

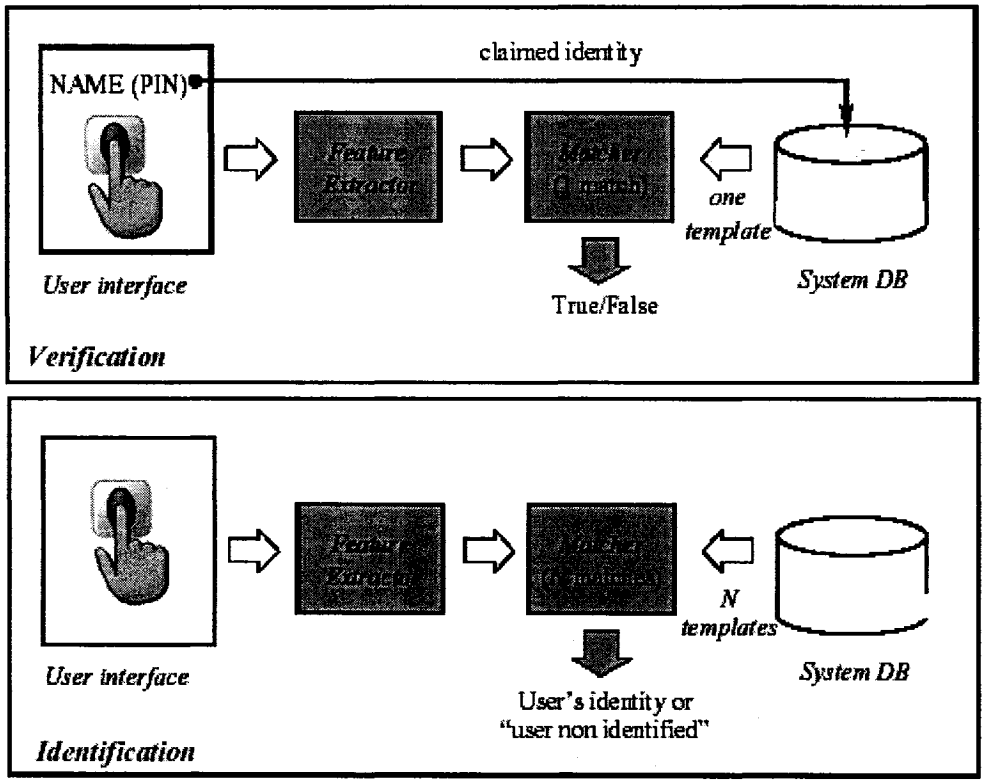

Figure 1.5 Block diagrams of verification and identification.

Another way of measuring performance uses Receiver Operating Characteristic (ROC). This curve (as shown in Fig. 1.7) is a plot of FRR (or the genuine acceptance rate, 100-FRR) against FAR for all possible operating points.

1.4. Biometrics Applications

Biometric systems have been used extensively (see Fig. 1.8) and some of their applications are listed below [2][6-11]:

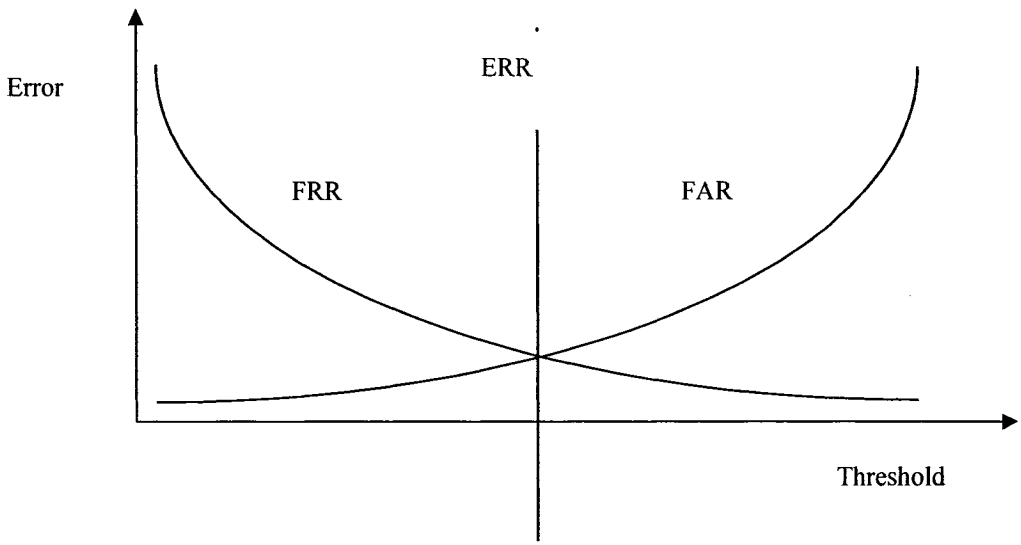

Figure 1.6 FRR, FAR and ERR.

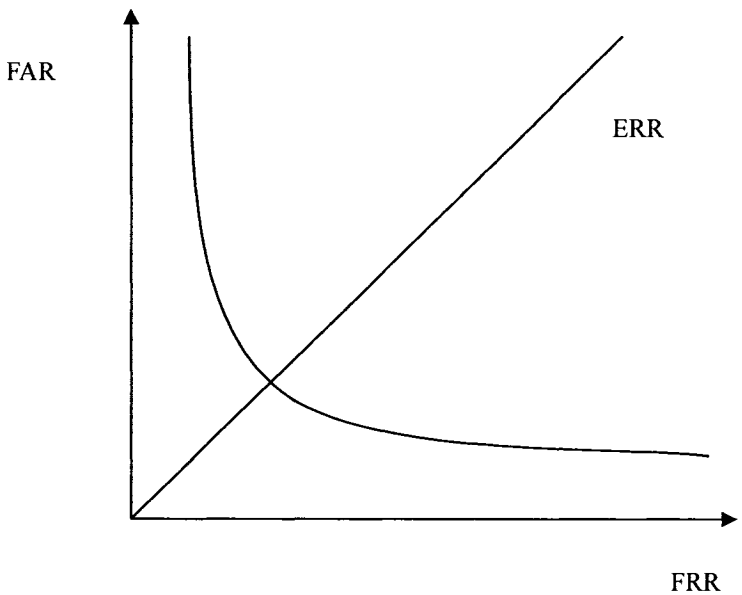

Figure 1.7 ROC curve.

Law Enforcement

The law enforcement community is perhaps the largest biometrics user group. Police forces throughout the world use AFIS technology to process criminal suspect, match finger images and bring guilty criminals to justice. A number of biometrics vendors are earning significant revenues in this area.

Banking

Banks have been evaluating a range of biometrics technologies for many years. Automated Teller Machines (ATMs) and transactions at the point of sale are particularly vulnerable to fraud and can be secured by biometrics. A variety of biometrics technologies are now striving to prove themselves throughout this range of diverse market opportunities.

Computer Systems

Biometrics technologies are proving to be more than capable of securing computer networks. This market area has phenomenal potential, especially if the biometrics industry can migrate to large-scale Internet applications. As banking data, business intelligence, credit card number, medical information and other personal data become the target of attack, the opportunities for biometrics vendors are rapidly escalating.

Physical Access

Schools, nuclear power stations, military facilities, theme parks, hospitals, offices and supermarkets, across the globe, employ biometrics to minimize security threats. As security becomes more and more important for parents, employers, governments and other groups - biometrics will be seen as a more acceptable and therefore an essential tool. The potential applications are infinite.

Benefit Systems

Benefit systems like welfare especially need biometrics to struggle with fraud. Biometrics is well placed to capitalize on this phenomenal market opportunity and vendors are building on the strong relationship currently enjoyed with the benefits community.

Immigration

Terrorism, drug trafficking, illegal immigration and an increasing throughput of legitimate travelers is putting a strain on immigration authorities throughout the world. It is essential that these authorities can quickly and automatically process law-abiding travelers and identify them. Biometrics are being employed in a number of diverse applications to make this possible. The US Immigration and Naturalization Service is

a major user and evaluator of a number of biometrics. Systems are currently in place throughout the US to automate the flow of legitimate travelers and deter illegal immigrants.

National Identity

Biometrics are beginning to assist governments as they record population growth, identify citizens and prevent fraud from occurring during local and national elections. Often this involves storing a biometrics template on a card that in turn acts as a national identity document. Finger scanning is particularly strong in this area and schemes are already under way in Jamaica, Lebanon, Philippines and South Africa.

Telephone Systems

Global communication has truly opened up over the past decade. While telephone companies are under attack from fraud. Once again, biometrics are being called upon to defend this onslaught. Speaker ID is obviously well suited to the telephone environment and is making in-roads into these opportune markets.

(a) Face recognition system

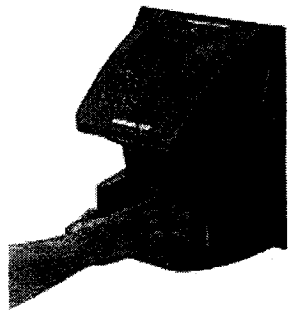

(b) HandPunch 2000

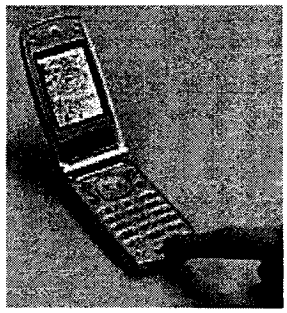

(c) Cellphone with fingerprint scanner

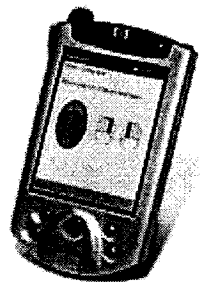

(d) PDA with fingerprint scanner

Figure 1.8 Biometric applications used in different sectors. (a) Face recognition system [32] used in law enforcement. (b) HandPunch 2000 [33] used in the corporate world. (c) and (d) Fingerprint scanner [34] found on personal electronic devices.

Time, Attendance and Monitoring

Recording and monitoring the movement of employees as they arrive at work, have breaks and leave for the day were traditionally performed by 'clocking-in' machines. Replacing the manual process with biometrics prevents any abuses of the system and can be incorporated with time management software to produce management accounting and personnel reports.

Table 1-1 lists some of the other various biometric applications.

Table 1-1 Overview of various biometrics applications.

Biometrics	**Applications**	**Summary of Applications**
Dental	Recognition	Forensics
DNA	Recognition	Forensics, medicine, genetics
Fingerprint	Recognition / Verification	Immigration & naturalization, welfare distribution, military identification, forensics, access control
Face	Verification / Recognition	Suspect description & identification, missing persons, licenses, credit card, welfare distribution
Hand	Verification	Access control, immigration & naturalization, services distribution
Signature	Verification / Recognition	Signature verification, Identification from handwriting
Iris	Verification	Access control
Voice	Verification/ Recognition	Speaker verification, phone service, speaker identification, access control

1.5. Thesis Organization

This thesis is organized in the following chapters. Some basic biometric concepts have been introduced in Chapter 1. Chapter 2 is a background study of line features in biometrics and some current line detection/extraction methods are also overviewed. In Chapter 3 we present our approach of line detection/extraction that includes wide information by Multi-scale Gaussian Filters (MGF). Chapter 4 and 5 discuss two applications where our method is used, personal authentication using palm veins and detection of Diabetic Retinopathy via retinal blood vessels. Finally the conclusion and discussion are presented in Chapter 6. Fig. 1.9 is the outline of the global structure of this thesis.

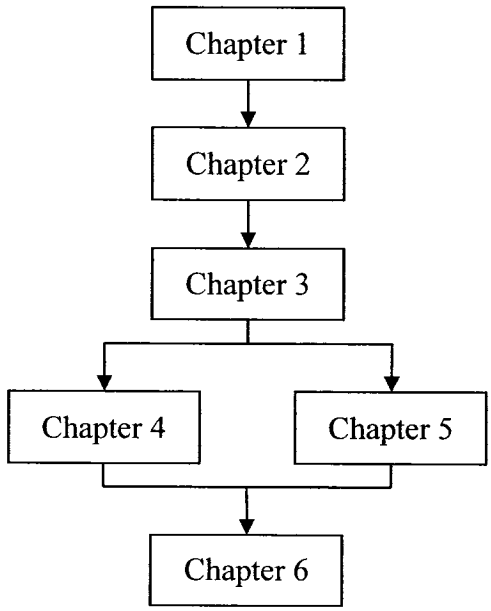

Figure 1.9 Structure of this thesis.

Chapter 2

Research Background

This chapter highlights the research background of this project on line feature extraction. An introduction is presented in Section 2.1. In Section 2.2 the three methods of traditional line extraction are given, which are Hough transform, Differential Geometry and Edge Extraction. Examples of application using line features are shown in Section 2.3 and the connection between lines and biometrics is made afterwards. The three methods previously mentioned do not consider a line's wide information which is important in biometrics. Two current line extraction methods (see Section 2.4) that retain the line's wide information are presented afterward and analyzed to indicate their shortcomings. Finally, a summary of this chapter is made by reiterating the importance of line features and their wide information in biometrics.

2.1. Introduction

Having given an overview of biometrics what is explained next is one of its features, lines, composed of edges. Awcock and Thomas define an edge in a digitized image as a sequence of connected edge points where an edge is characterized by an abrupt

change in intensity indicating the boundary between two regions in an image [35]. A line according to their definition is a region of constant intensity found between two edges which act as a boundary for the line.

Line detection in digital images is an essential operation in image analysis as well as computer vision and plays an important role for the success of higher-level processing such as matching and recognition [36-41]. In photogrammetric and remote sensing tasks it can be used to extract linear features such as roads, railroads and rivers from satellite or low-resolution aerial imagery which can be used for the capture or update of data for geographic information systems [42]. It is also extensively used in medical imaging for extracting anatomical features such as linear structures in mammograms [43], blood vessels from an X-ray angiogram [44] or a retina image [45], the bones in the skull from a CT or MR image [46] and cracks on a tongue surface in TCM [47]. In addition, line detection is useful in for example, extracting strokes in character recognition [48-49], in estimating motion and structure from multiple images [50-51] and in detecting biometric traits for personal authentication [52]. Some of the typical line features are illustrated in Fig. 2.1. There are three main traditional line detection methods which can used to detect the various applications mentioned above and are introduced next.

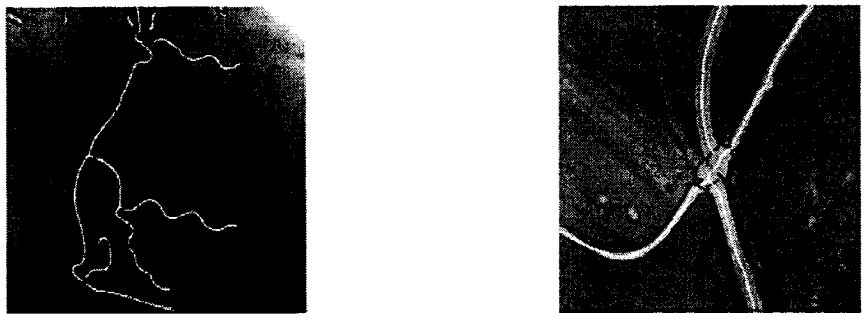

(a) (b)

Figure 2.1 Images that contain line features. (a) X-ray. (b) Satellite imagery of countryside road.

2.2. Traditional Line Feature Extraction Methods

Method 1: Hough Transform

Hough transform [53-55], which is a widely used line detection method, was initially proposed to find analytically defined curvilinear structures (e.g., straight lines, circles, ellipses etc.). It transforms the equation of a line in the form $y = mx + b$ into parameters (p, θ) where p is the smallest distance between the line and the origin and θ is the angle of the locus vector from the origin to the closest point (see Fig. 2.2).

From this parameterization, the equation of the line can be rewritten as:

$$p = x\cos\theta + y\sin\theta \tag{2.1}$$

Points on the same line in the image space once transformed into sinusoids will cross at the parameters (p, θ) for that line. This essentially translates the problem of

detecting colinear points into the problem of finding concurrent curves. Generalized Hough transform [57] which was developed afterwards can be used to detect arbitrary line structures in theory but requires a complete specification of the exact shape of this structure.

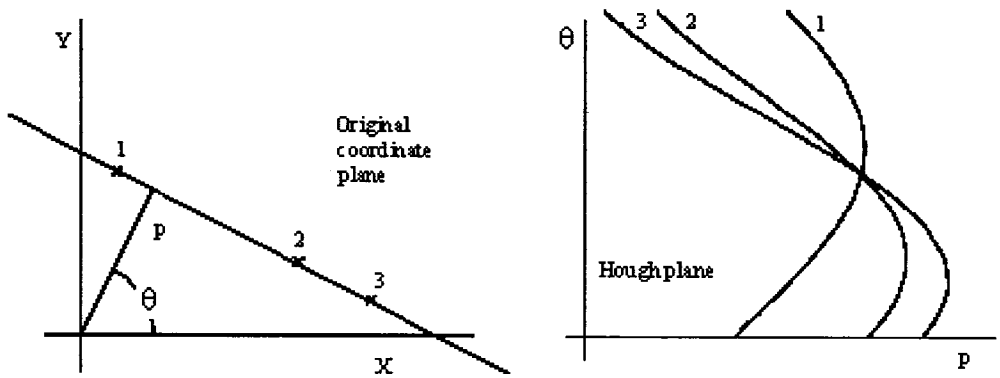

Figure 2.2 Original coordinate plane and corresponding Hough plane [56].

The problem with Hough transform is that it's difficult and even unfeasible at times for complex models to be represented in practice. This is because *(p, θ)* have to be calculated for every point which takes up too much computation time for large images.

Method 2: Differential Geometry

One popular method is to use differential geometric properties to extract lines as ridges and valleys in the image [58-63]. A useful ridge detector [64] is based on the

eigenvectors of the Hessian matrix which is given by the local second order derivatives. This detector extracts the ridges as points for which the intensities are maxima or minima in the main principal curvature direction, i.e., the direction of the maximum eigen-value of the Hessian matrix [65]. Nevertheless, this method is sensitive to noise due to the use of second order of derivatives.

Method 3: Edge Extraction

Another powerful method is based on edge extraction and treats lines as objects with parallel edges [66-71]. Canny [72] came up with an edge detection method that many regard as an optimal edge detector. He addressed the issues and shortcomings of other edge detectors at the time. They were, reducing the error rate, localizing edge points and finally having only one response to a single edge. The first step of Canny's method was to remove noise and smooth the image using a Gaussian filter. Next the gradient of the image (edge strength) was calculated by applying Sobel once for the x-axis, the other for the y-axis and then taking their sum.

$$|G| = |Gx| + |Gy| \tag{2.2}$$

The third step involves finding the direction of the edge which can be computed as:

$$\theta = \tan^{-1}(Gy / Gx) \tag{2.3}$$

In the fourth step the method takes the direction of the edge just calculated and decides how it relates back to the image so it can be traced. Step five goes along the edge and finds pixels not considered an edge and sets it to 0. Finally, in the last step hysteresis is applied to remove any streaking in the image.

2.3. Applications Using Line Features

Due to the popularity of the edge extraction method, some applications based on it are given below.

Line Feature of Knuckleprint

Six steps are applied to extract line features after they are located on the knuckle [73].

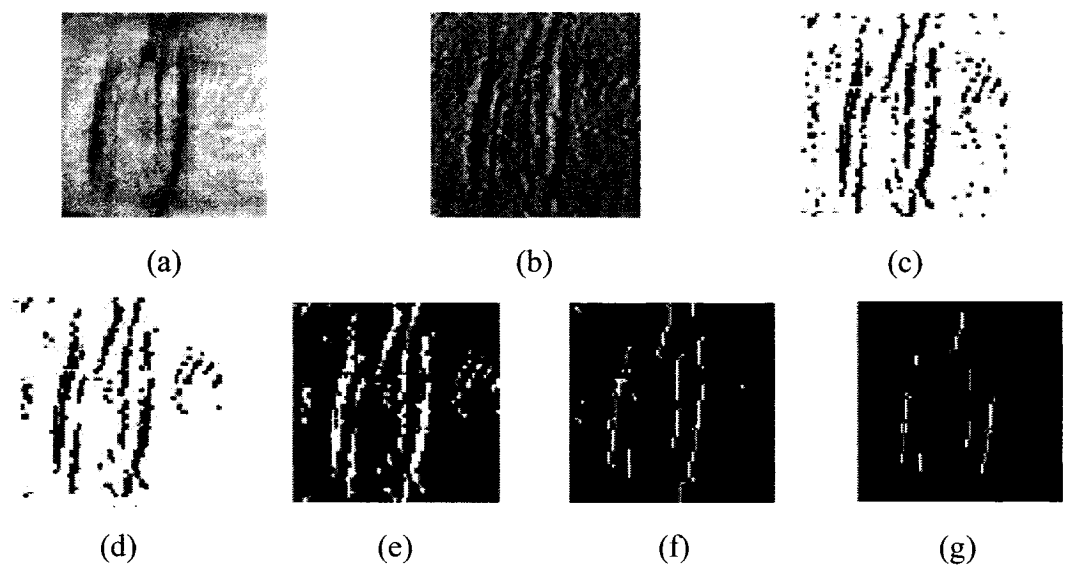

Figure 2.3 Knuckleprint feature extraction [73].

The first step is convoluting the ROI (Region of Interest) seen in Fig. 2.3(a) with a 1x7 mask H, where:

$$H = [-1, -1, -1, 6, -1, -1, -1] \tag{2.4}$$

The result after convolution shown in Fig. 2.3(b) enhances lines. The next step involves applying a threshold $T = 50$ to the masked image (Fig. 2.3(c)). Any point whose value is greater than T is considered on the line while those that are less than T are not and set to 0. The third step reduces noise using a 2-D adaptive wiener filter (see Fig. 2.3(d)). In step four another threshold T is employed but this time is set to 150. Anything greater than 150 is assigned 0 otherwise the value 1. This transforms the gray-scale image into a binary one (Fig. 2.3(e)). A set of morphological operations are used in step five (Fig. 2.3(f)). Finally in the last step the most significant lines are preserved by reducing the shorter lines and condensing the longer ones as seen in Fig. 2.3(g).

Line Feature of Palmprint

Wu et la. [74] devised a way to detect the principal lines (life line, head line and heart line) and wrinkles of a palm that can be used to identify an individual. They defined principal lines and wrinkles as edges, but can not detect their direction. [74] gives a

solution to solve this problem by introducing θ- directional line detectors which detects lines in θ direction.

Fig. 2.4 shows some examples of the extracted palm-lines in which (a) is the original palmprint images; (b) is the extracted palm-lines and (c) is the palmprint images overlapped with the extracted palm-lines. In these examples, θ = 0°-, 45°-, 90°- and 135°- directional line detectors are used for palm-line extraction.

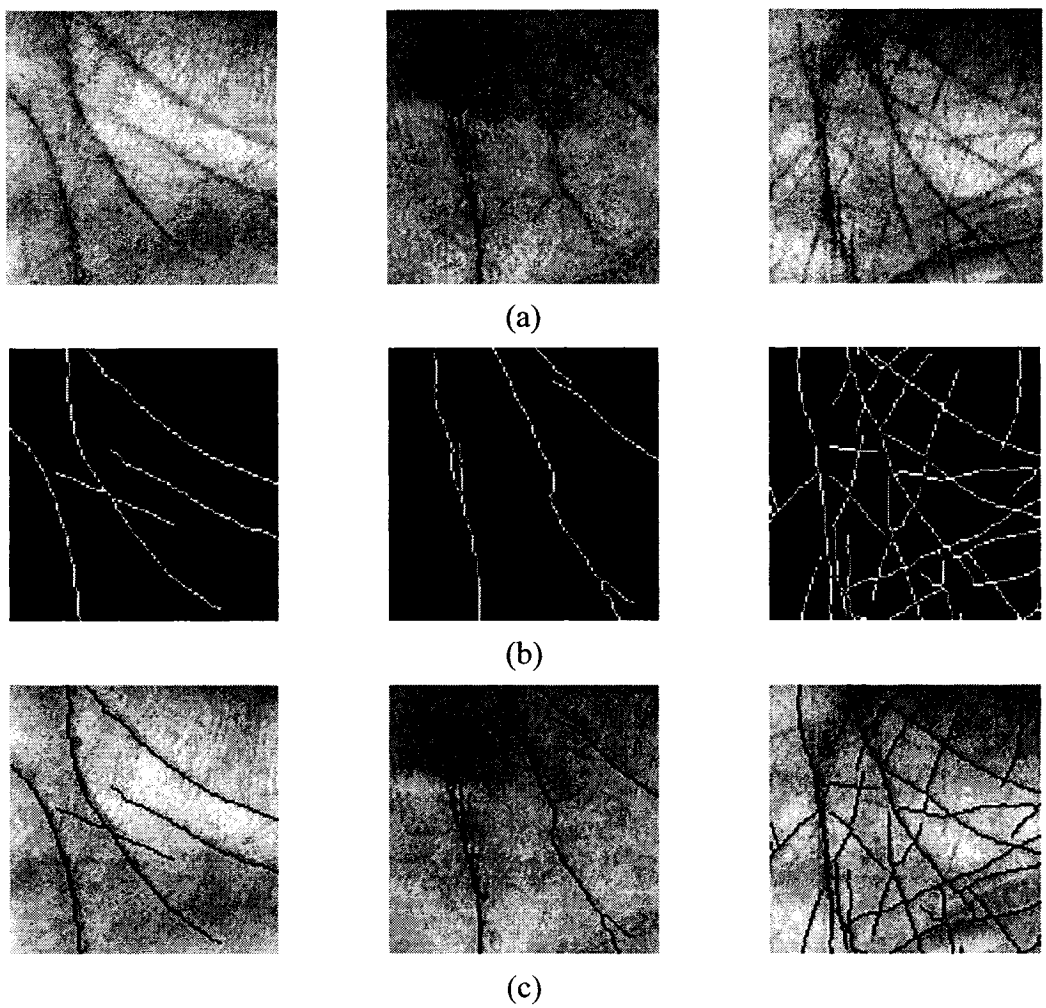

Figure 2.4 Some results of palm-line extraction. (a) Original images, (b) extracted palm-lines, (c) the palmprint images overlapped with the extracted palm-lines.

Line Feature in Back of the Hand

Wang et la. [77] proposed a new personal verification system using thermal-imaged vein patterns in the back of the hand (Fig. 2.5). To capture vein patterns they used an NEC Thermal Tracer. The ROI is defined as a rectangular region in the hand image and is located using the same technique developed by Lin and Fan [78]. Once the ROI is extracted a 5x5 median filter is applied to the image to remove speckling noise.

Figure 2.5 Thermal images of back of the hand.

A 2-D Gaussian low pass filter is then utilized to subdue the effect of high frequency noise (Fig. 2.6).

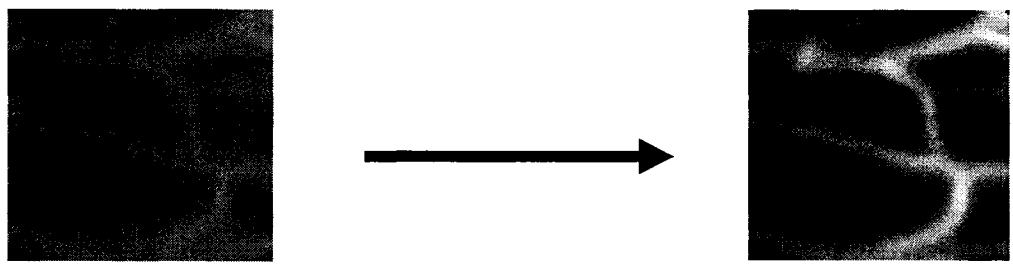

(a) (b)

Figure 2.6 Edge enhancement. (a) Original image and (b) The image after removing noise.

In order to extract the vein patterns local thresholding (Fig. 2.7) and skeletonization (Fig. 2.8) are used. Local thresholding separates the vein pattern from its background and different threshold values exist for every pixel based on its neighborhood. More precisely the threshold of every pixel is equal to the mean of its 13x13 neighborhood.

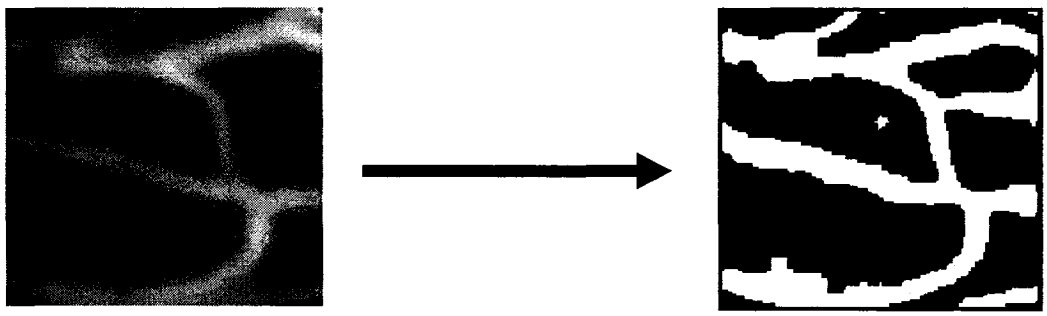

(a) (b)

Figure 2.7 Binarising operation. (a) Original image and (b) Binary image by local thresholding.

After the pattern is skeletonized, Zhang and Suen's [79] thinning algorithm is applied to obtain an image where the vein patterns are clearly distinguishable.

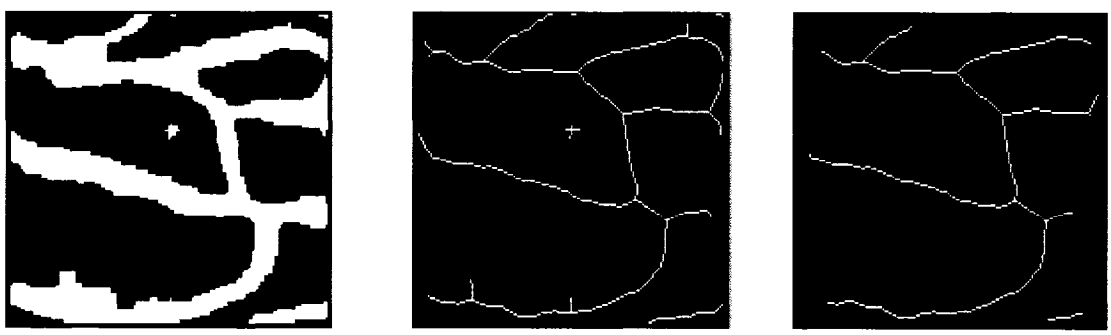

(a) (b) (c)

Figure 2.8 Skeletonization operation. (a) Original image; (b) Thinned image; and (c) the image after pruning to remove spur branches and cleanup isolated pixels.

2.4. Extracting Lines with Wide Information

Three different methods defined in Section 2.2 can detect line existence and structure without wide information. As you can see, some examples of their applications (introduced in Section 2.3) illustrate this corresponding result. However, some biometric characteristics with wide line information are very useful and important. If the line widths of these characteristics are included in a biometric system, more accuracy is guaranteed to better identify individuals. For example, palm vein and retina images in Fig. 2.9 not only tell us if a line exists but also shows the width of this line. Therefore, it is necessary to develop algorithms which can detect/extract line feature with wide information for biometric applications.

(a) (b)

Figure 2.9 Biometric characteristics that contain line features and wide information. (a) Palm veins. (b) Retinal blood vessels.

Recently, Koller et al. [85] presented an algorithm for line, width and height detection using filters. This technique uses the first derivative of Gaussian to produce

edge detectors for the left and right edge. The results of the detectors are then combined using a nonlinear minimum function. Line width is calculated by iterating through the scale-space and selecting the scale that produces the maximum of a scale-normalized response. The problems in [85] are computationally expensive and the line width estimated will only be coarse.

Steger [42] proposed a ridge-based line detector which uses a line model with an asymmetrical profile to remove the bias of the line position as well as to extract the line width. This line detector overcomes the problem that the ridge-based line detection approach will return inaccurate line locations when the contrast on one side of the line is different from the contrast on the other side of the line. A limitation of [42] is that it can only detect lines between 0 and 2.5σ. This will be a concern if important lines exceed 2.5σ.

Thus, these two algorithms are insufficient for biometrics even though they detect the whole of the line. A line, mathematically, is a one-dimensional figure without thickness, but an image line generally appears as a line of one or several pixels wide, i.e., as a thin/narrow or thick/wide line, having linear or curvilinear structures. In biometric applications, line thickness or a line's full cross-section is important in, for example, segmenting multiple orientation lines [75], and in detecting biometric traits for personal authentication [52]. It is thus important to detect not

simply the line edges but rather the whole of the line.

Having established the importance of line and line width in biometrics, the next chapter will propose our approach of line detection/extraction which preserves wide information.

2.5. Summary

In this chapter, we analyze that line features can be used as a biometrics trait to identify individuals. A line's wide information is essential in biometrics and should be extracted in order to better recognize and match templates. Unfortunately, the tradition line extraction methods cannot retrieve this information. Even using current line extraction methods with wide information will not work well due to the method's shortcomings. As a result, it is necessary to develop a new approach to not only extract a line's existence and structure but also detect its wide information.

Chapter 3

Multi-scale Gaussian Filter (MGF)

This chapter proposes our approach to detect/extract lines with wide information. Some terminologies used in our approach are defined in Section 3.1. Section 3.2 describes the Gaussian filter which is the basis of our approach while Section 3.3 explains in detail the Multi-scale Gaussian Filter (MGF). We conclude with Section 3.4 in which a summary of our approach is given.

3.1. Introduction

Having established the need for a method to detect wide information from the previous chapter, we will introduce our approach in this one. Before that, some terminologies that will be used in following sections are defined below.

Cross-section

The Oxford English Dictionary defines cross-section (Fig. 3.1) as, "The cutting of anything across; a section made by a plane cutting anything transversely." As some examples, Fig. 3.7 shows the cross-sections of both palm veins and retina vessels. We can calculate the cross-section of a line in a gray-scale image by drawing a straight

line (Fig. 3.1(a)) through it and then for each pixel plot its gray-scale value (Fig. 3.1(b)). This graph will resemble a Gaussian shape as edges of the line are black while the middle is white. The purpose of using cross-section is that they represent the width of the line.

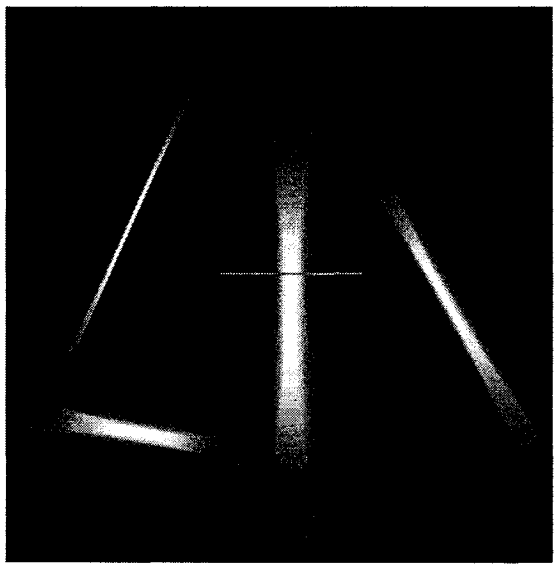

(a)

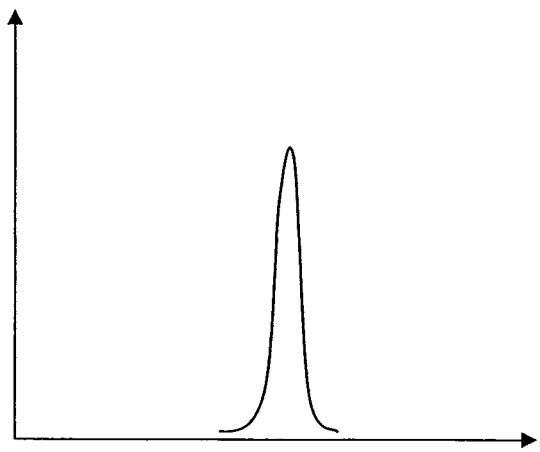

(b)

Figure 3.1 (a) Cross-section of a line and (b) its graph which resembles a Gaussian shape.

Noise

Noise exists in all forms in image acquisition and cannot be predicted due to its random nature. Noise is represented as high frequencies or rapid fluctuations in the image brightness graph. Fig. 3.2 shows a signal with and without noise.

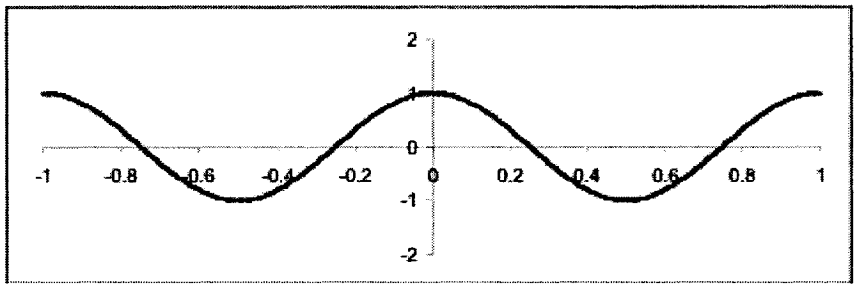

(a)

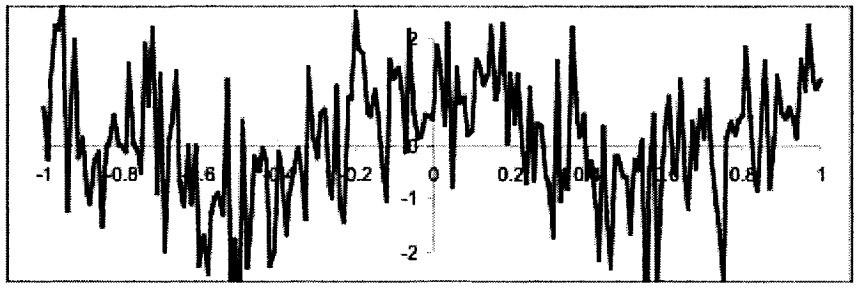

(b)

Figure 3.2 A signal (a) without noise and (b) with noise [86].

Histogram Equalization

This is a common preprocessing step that redistributes the histogram values (pixel values) in order to produce a more uniform histogram. As an example, the results before and after using histogram equalization are shown as in Fig. 3.3(a) and Fig.

3.3(b), respectively. Their corresponding histograms are also given in Fig. 3.4. The advantage of doing this is that the contrast in the original image is not so great anymore. John C. Russ [87] describes this process, "Histogram equalization reassigns the brightness values of pixels based on the image histogram. Individual pixels retain their brightness order (that is, they remain brighter or darker than other pixels) but the values are shifted, so that an equal number of pixels have each possible brightness value. In many cases, this spreads out the values in regions where different regions meet, showing detail in areas with high brightness gradient."

The key for this algorithm is the transfer function which converts the original histogram into one that is equalized. The transfer function we used can be defined as follows:

$$N_P = \frac{M \times N}{G} \tag{3.1}$$

$$i = MAX\left\{0, \text{round}\left(\frac{CH(j)}{N_P}\right) - 1\right\} \tag{3.2}$$

$$CH(J) = \sum_{j=0}^{J} N_j \tag{3.3}$$

where:

$M \times N$ is the size of the image;

G is the number of gray-scale levels;

N_P is the ideal number of pixels for each gray-scale level;

$CH(J)$ is the cumulative number of pixels at each gray-scale;

i is the result.

It is clear that we get a better quality image using the histogram equalization algorithm as can be seen from Fig. 3.3(a) to Fig. 3.3(b).

(a) (b)

Figure 3.3 (a) Before and (b) after pictures of histogram equalization.

Thresholding

Binary images are easier to analyze than grey-scale images, but often cannot be converted directly without some preprocessing. Hence, there is a need to threshold grey-scale images to obtain its binarised version where foreground and background regions can be segmented. A threshold value T is used to accomplish this by

partitioning the grey-scale image pixels to two values (0 and 1), using the following algorithm:

$$\text{IF } f(x,y) \geqq T \text{ THEN } b(x,y) = 1 \tag{3.4}$$

$$\text{ELSE } b(x,y) = 0 \text{ since } f(x,y) < T \tag{3.5}$$

where $f(x,y)$ denotes the original grey-scale image and $b(x,y)$ denotes the binarised version of $f(x,y)$.

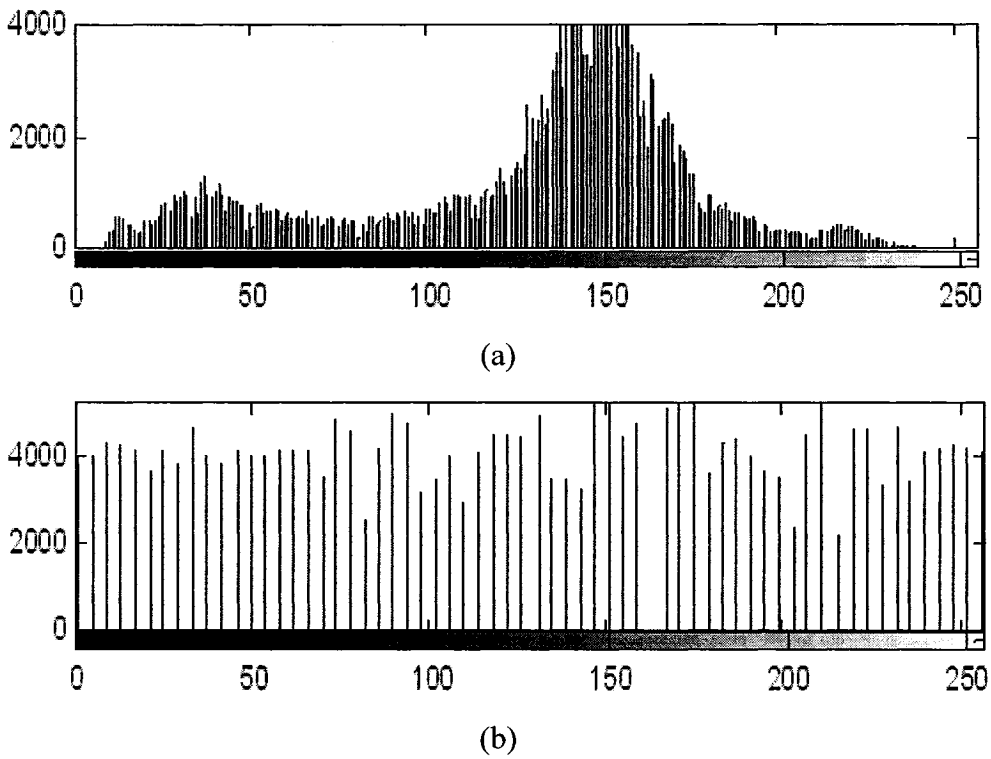

Figure 3.4 (a) Before and (b) after image histograms corresponding to Fig. 3.3.

The selection of T is an important issue and a common way is by looking at the image histogram. An image which features two or more clearly marked peaks separated by troughs is appropriate for binarisation. Bimodal histogram (Fig. 3.5) is the classic example of this. In this case, T is the lowest point of the trough (*T1* in Fig. 3.5). Another example is the dual threshold, as shown in Fig. 3.6. Here two thresholds are defined by looking for troughs, i.e., any value between *T1* and *T2* is set to 1 while everything else to 0.

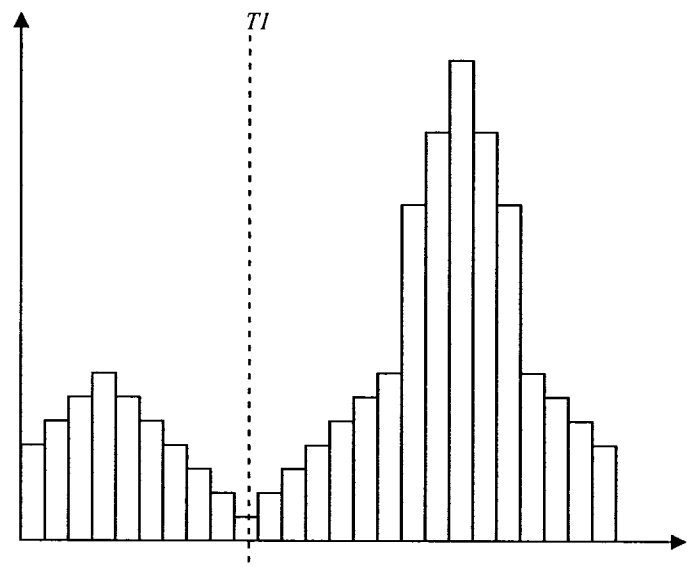

Figure 3.5 Bimodal histogram where *T1* is defined as the threshold.

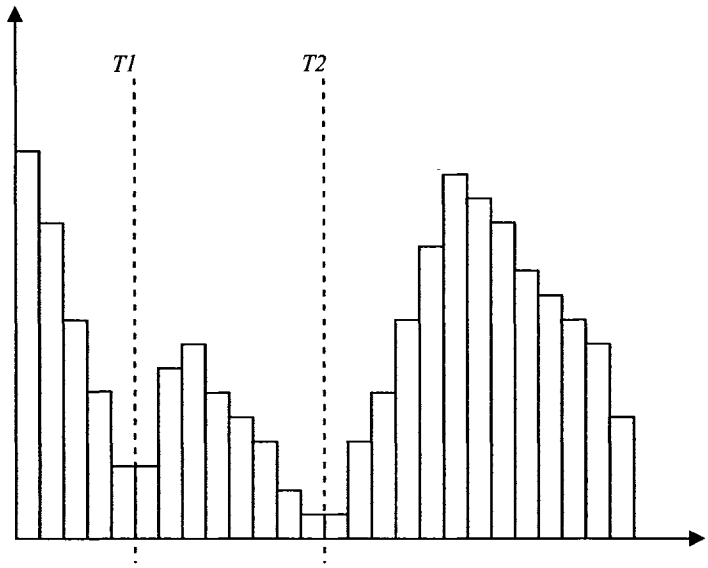

Figure 3.6 Dual thresholding where *T1* and *T2* are the thresholds.

3.2. Gaussian Filter

Gaussian filter is commonly used in image processing to smooth an image. This is achieved by changing the convolution mask coefficients such that a suitable degree of precision is preserved within the smoothed image. An advantage of the Gaussian filter is that the mask is rotationally symmetric. This means there will be no directional bias in the amount of smoothing that is carried out. Image smoothing seeks to remove unnecessary noise from the image while simultaneously preserving the essential details.

Detecting a line by Gaussian Filter

First of all, we observe the cross-section of a given subject to decide if it is a Gaussian

shaped line. As an example, two kinds of biometric lines, palm veins and retinal blood vessels, are indicated in Fig. 2.9. By examining their cross-sections, Fig. 3.7(a) shows the intensity distribution of retinal vessel cross-sections for both small vessels and large vessels and Fig. 3.7(b) shows some cross-sections of the palm veins. Based on the observation that the cross-sections of these lines are similar to Gaussian, a Gaussian shaped filter proposed in [45] [84] can be used to detect them. There are two common Gaussian Filters: 1-D and 2-D. They are introduced below.

1-D Gaussian Filter

A 1-D Gaussian function is given as:

$$g(x) = \frac{1}{\sqrt{2\pi\sigma}} \exp\left(-\frac{x^2}{2\sigma^2}\right) \tag{3.6}$$

where σ is the standard deviation of the Gaussian function and is illustrated by Fig. 3.8, two 1-D Gaussian curves are given with their corresponding data values ($\sigma = 2$ and $\sigma = 3$).

Notice that σ controls the degree of smoothing of the Gaussian curve. The greater the value of σ the larger the smoothing and the more the image is blurred. On the other hand a small value of σ will mean less smoothing while fine details are retained.

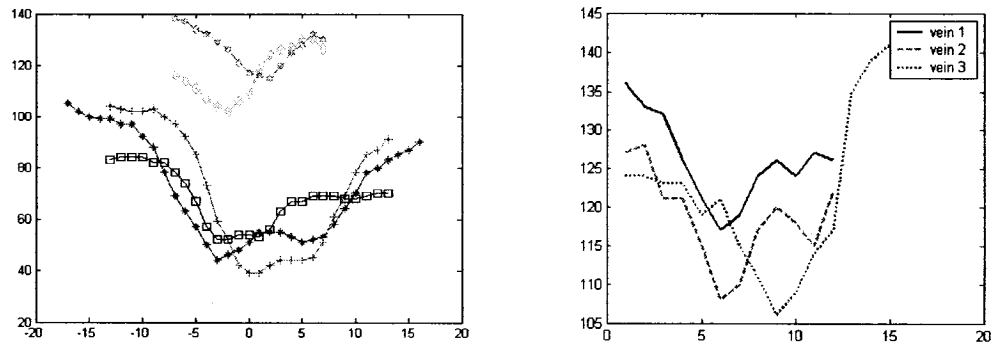

(a) (b)

Figure 3.7 Samples of cross-sections from Fig. 2.9. (a) Intensity distribution of retinal vessel cross-sections for both small vessels and large vessels. (b) Cross-section of palm veins.

2-D Gaussian Filter

A 2-D Gaussian function is defined in the following as:

$$g(x,y) = \frac{1}{2\pi\sigma^2}\exp\left(-\frac{x^2+y^2}{2\sigma^2}\right) \tag{3.7}$$

Fig. 3.9 illustrates a 2-D Gaussian curve. In our approach the Gaussian filter has two parameters, σ (referred to as scale) and ϕ (referred to as orientation). A complete explanation of this approach is developed in the next section.

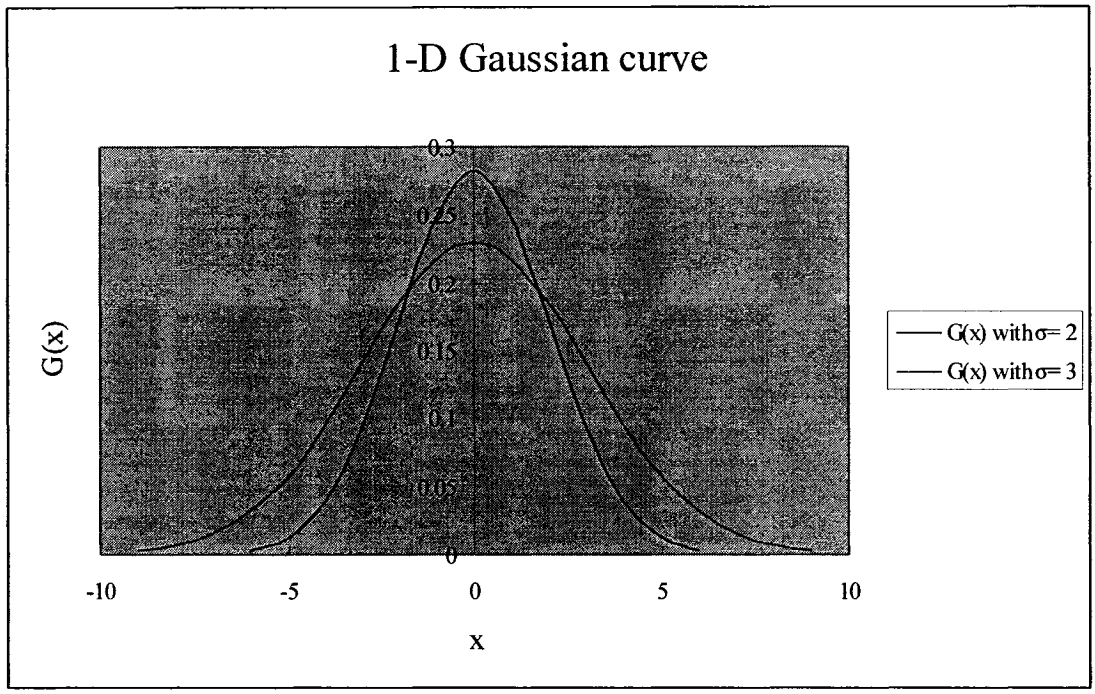

0.003	0.012	0.038	0.092	0.171	0.249	0.282	0.249	0.171	0.092	0.038	0.012	0.003

$\sigma = 2$

0.03	0.07	0.15	0.31	0.57	0.95	1.4	1.84	2.18	2.30	2.18	1.84	1.40	0.95	0.57	0.31	0.15	0.07	0.03

$\sigma = 3$ (to obtain actual values x 0.1)

Figure 3.8 1-D Gaussian curve.

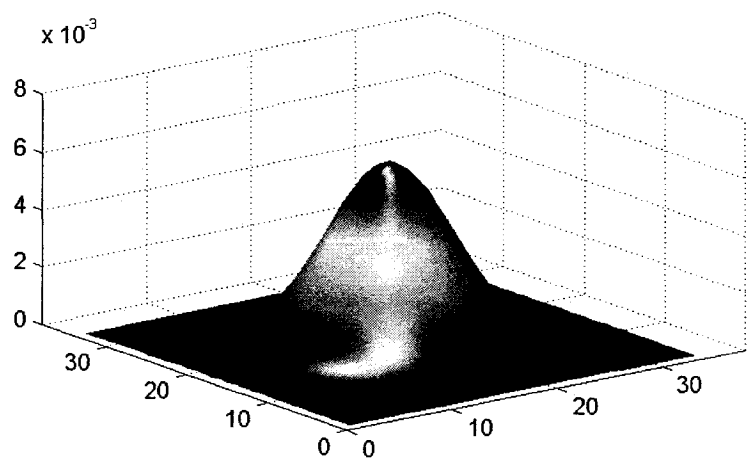

Figure 3.9 2-D Gaussian curve [88].

3.3. MGF Design

Single Gaussian Filter

The single Gaussian filter can be defined as:

$$g(x,y) = -\exp\left(-x^2/\sigma^2\right) - m, \quad \text{for } |x| \le 3\sigma, \quad |y| \le L/2 \tag{3.8}$$

where σ represents the scale of the filter; $m = -\left(\int_{-3\sigma}^{3\sigma} \exp\left(-x^2/\sigma^2\right)dx\right)/6\sigma$ is used to normalize the mean value of the filter to 0 so that the smooth background can be removed after filtering; L is the length of the neighborhood along y-axis to smooth noise. In practice, we will rotate $g(x,y)$ to detect the vessels of different orientations. The rotation of $g(x,y)$ with angle ϕ is

$$\begin{cases} g^{\phi}(x',y') = g(x,y) \\ x' = x\cos\phi + y\sin\phi \\ y' = y\cos\phi - x\sin\phi \end{cases} \tag{3.9}$$

There are a total of 24 single Gaussian Filters, one for each scale (a total of three) and direction (a total of eight) as can be seen from Fig. 3.10. Normally, we choose three (large, medium and small) scales based on the cross-section of lines analyzed. The widest cross-section is assigned the largest scale, the thinnest the smallest and the third scale (medium) is calculated by taking the average of the other two (largest and smallest). Eight directions are chosen to cover all possible orientations of the line,

including horizontal, vertical and diagonal.

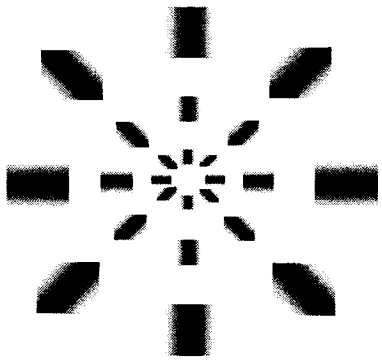

Figure 3.10 Single Gaussian filter design at three different scales and eight directions.

In some applications we cannot get a good result using only a single Gaussian filter. As an example, Fig. 3.11 emulates line detection via single scale filters, $g(x,y)$, where s is the original signal of several cross-sections of lines with different widths and f is s with background noise added. The response of $g(x,y)$ to $f(x,y)$ is

$$R(x,y) = g(x,y) * f(x,y) \tag{3.10}$$

where $*$ is convolution. Three different responses, R_1, R_2 and R_3, are given by the three different single Gaussian filters. As can be seen in this figure, a small scale response (R_1) can detect lines of small widths but cannot detect lines of larger widths or remove noise effectively. On the other hand, a large scale response (R_3) can detect wide lines but cannot detect thin lines because they are smoothed too much. Using (R_2) also does not work. The question that remains to be answered, is there a way to

detect small to large widths while at the same time suppress noise?

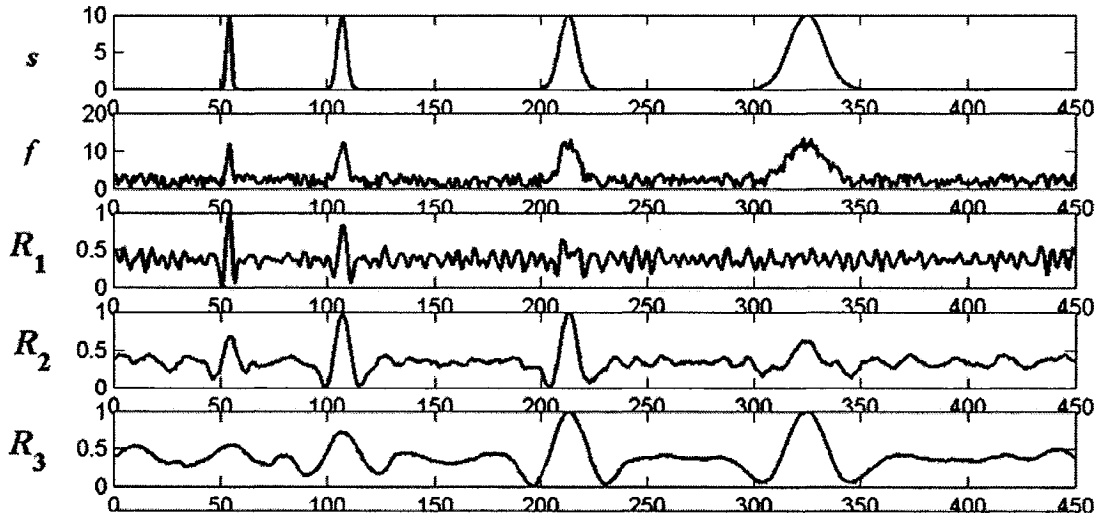

Figure 3.11 Responses of single scale filters, where s is the original signal, f is the noisy measurement of s, and R_1, R_2 and R_3 are the single Gaussian filter responses to f at different scales.

Multi-scale and Scale Production

From Fig. 3.11 we found that there is too much noise in the single Gaussian filter responses. To gain a proper signal-noise ratio, we propose a multi-scale scheme to detect line features. In [89], Mallat illustrated mathematically that signals and noise have different singularities and that edge structures present observable magnitudes along the scales, while noise decreases rapidly. With this observation, we respond to the problems of edge/line detection and noise reduction by thresholding the multi-scale products [90-92].

Multi-scale

As the name suggests, multi-scale refers to more than one scale. The purpose of using this idea is to detect common features in images scaled with different values. On way of doing this is first apply a small scale to the original image in order to extract edge details and then use a larger scale on the same image to extract the general shape of the object. The scaled images are then examined looking for zero crossings present in both.

Multi-scale production

Fig. 3.12 illustrates the steps of our MGF. After image capture and histogram equalization, the different Gaussian filters, g_1, g_2, ... , g_N, are applied in parallel. The responses of these Gaussian filters at different scales and different orientations are then computed followed by scale production.

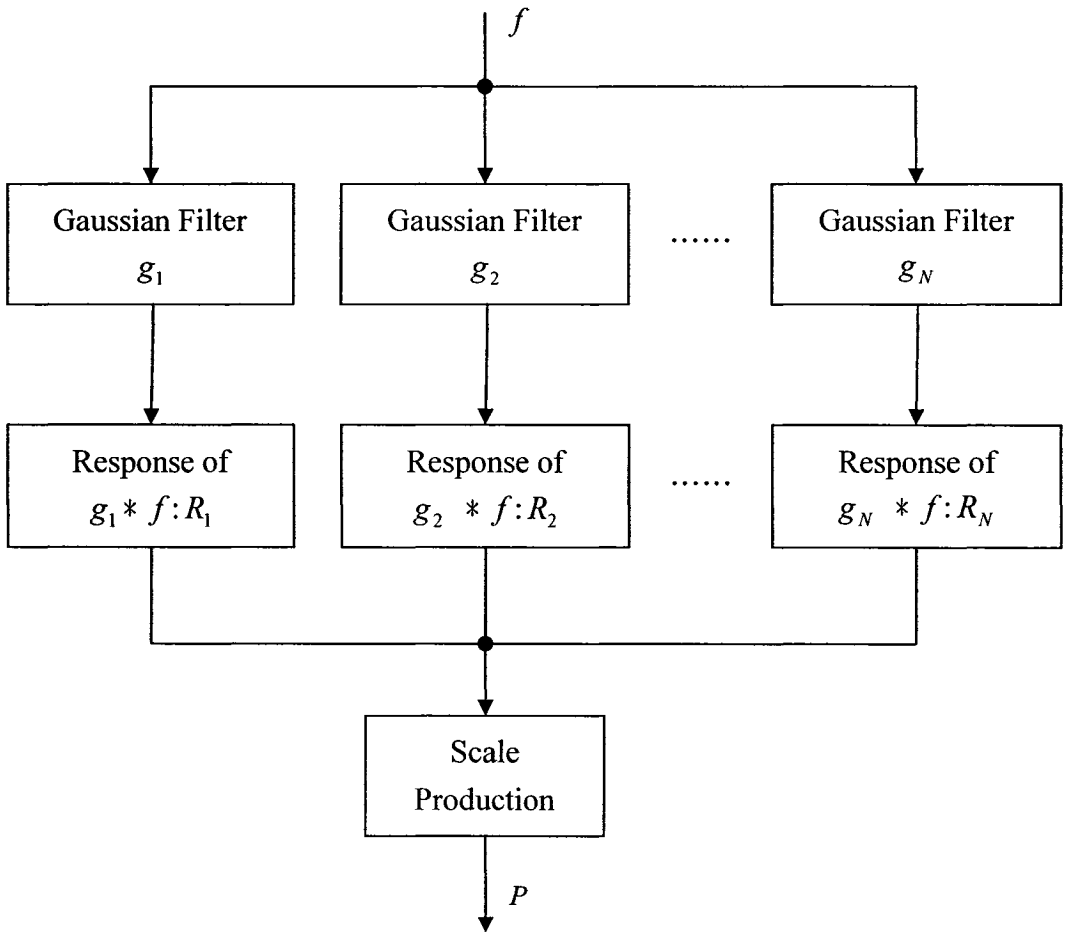

Figure 3.12 Steps of the Multi-scale Gaussian Filter.

The multi-scale filter is defined as:

$$g_i(x,y) = -\exp\left(-x^2/\sigma_i^2\right) - m_i, \quad \text{for } |x| \le 3\sigma_i, \quad |y| \le L_i/2 \tag{3.11}$$

where σ_i is the standard deviation of the Gaussian function at scale i. Correspondingly, $m_i = -\left(\int_{-3\sigma_i}^{3\sigma_i} \exp\left(-x^2/\sigma_i^2\right)dx\right)/(6\sigma_i)$, and L_i is the length of the filter in y direction at that scale. The rotation of $g_i(x,y)$ with angle ϕ is then implemented by using $g_i^{\phi}(x',y') = g_i(x,y)$, where

$x' = x\cos\phi + y\sin\phi$ and $y' = y\cos\phi - x\sin\phi$. Here we continue to use 3 scales and 8 directions from Fig. 3.10. Without loss of generality and for the convenience of expression, we discuss only the multi-scale filter in the horizontal direction. The filters in other directions can be derived similarly. The response of a filter $g_i(x,y)$ to an input image $f(x,y)$ can be expressed by

$$R_i(x,y) = g_i(x,y) * f(x,y) \tag{3.12}$$

where $*$ is convolution. The scale production is defined as the product of filter responses at different scales

$$P_{i,j}(x,y) = R_i(x,y) \cdot R_j(x,y) \tag{3.13}$$

where $i,j=1, 2, ..., N; i \neq j$ and dot represents multiplication. The image pixels in the response are first normalized and then multiplied together. This is simply done by dividing every pixel by 255 (to obtain a value from 0 to 1) and then multiplying corresponding pixels from the N responses. Each pixel is then converted back to 0-255.

Taking Fig. 3.11 as an example, Fig. 3.13 is its extension with the addition of three graphs. *Max* is a commonly used technique to select the response with maximum output from R_1, R_2 and R_3. $P_{1,2}$ is the scale production of R_1 and R_2, and

$P_{2,3}$ is the scale production of R_2 and R_3. As you can see $P_{1,2}$ and $P_{2,3}$ detect the cross-sections of s more accurately than any of the single scale responses and is also better at denosing. Of course the *Max* rule can also be used to fuse multi-scale responses [85][93], but as seen in Fig. 3.13 though both the large and small width vessels can be picked up, too much noise is preserved. This demonstrates the value of our multi-scale production approach.

After scale production we use double thresholding to distinguish line features from noise. This also helps us to create a binarised image. For double thresholding a low threshold t_l and a high threshold $t_h = 2t_l$ are imposed on a production where two maps V_l and V_h are obtained. The values in the production below t_l are removed as noises (set the value 0 in the binary image) and the remaining (set to the value 1 in the binary image) are extracted as line features to V_l. The same procedure is applied for $t_h = 2t_l$ however, this time values above t_h are removed as noises while values below t_h are placed in V_h. The final map is formed as the intersection of V_l and V_h. This process is repeated for each production using the same thresholds. The final binary image is attained by fusing every production's final map with logical OR.

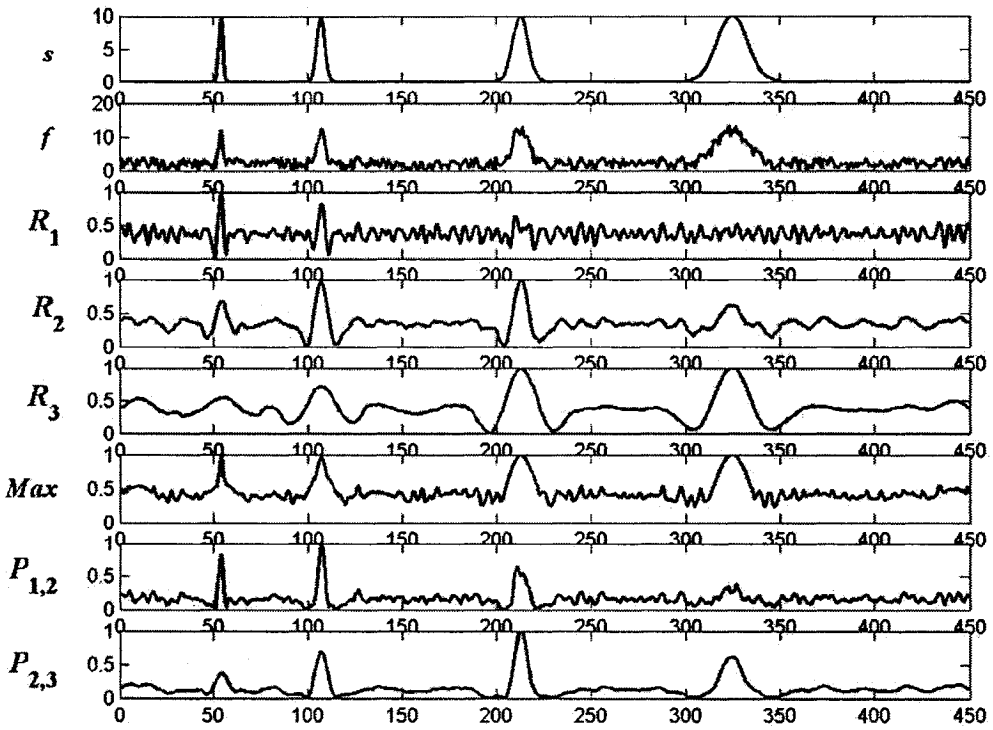

Figure 3.13 Multi-scale filters and scale production: s is the original signal; f is the noisy measurement of s; R_1, R_2 and R_3 are the filter responses to f at different scales; *Max* means the maximum values among R_1, R_2 and R_3; $P_{1,2}$ is the scale production of R_1 and R_2, and $P_{2,3}$ is the scale production of R_2 and R_3.

3.4. Summary

By using a single scale filter a lot of noise is produced which can be resolved using a multi-scale approach. In this chapter the proposed Multi-scale Gaussian Filter is designed with two parameters, scale σ and direction ϕ. This filter may use three scales based on the cross-sections of line widths and eight directions. Combining two responses using different scales forms a scale production. Thresholding is then

applied to the production to distinguish between useful features and non-useful parts. Using this technique a line's wide information is preserved as this is embedded into the image. The proceeding chapters demonstrate two applications where our approach can be applied, palm vein (see Chapter 4) and retinal blood vessels (see Chapter 5).

Chapter 4

Case Study 1:
Palm Vein Recognition

This chapter presents our case study of palm vein recognition using the proposed line feature extraction approach [94]. Since the vein information represents the liveness of humans, this system can provide personal authentication and liveness detection concurrently. In Section 4.1 we explain infrared palm images capture followed by detection of region of interest (Section 4.2). Section 4.3 discusses palm vein extraction by multi-scale filtering and Section 4.4 describes the matching technique used. Experimental results and a summary of our application are given in Sections 4.5 and 4.6 correspondingly.

4.1. Infrared Palm Images Capture

The capture device we used was modified from the previous work on palmprint [26]. Fig. 4.1(a) shows part of the device. There are three poles to help the user fix his/her hand (Fig. 4.1(b)). A low cost CCD camera is used in this system in order to obtain infrared images and an infrared light source is installed around the camera.

(a) (b)

Figure 4.1 Capture device: (a) Outside of the device and (b) Poles to fix a palm.

4.2. Detection of Region of Interest

After image capture and image preprocessing (histogram equalization), the region of interest (ROI) is located by the same method used in [26]. A small area (128*128 pixels) of a palm image is defined as ROI in order to extract the features and to compare different palms. Using the features within ROI for recognition can improve the computation efficiency significantly. Further, because this ROI is located by a normalized coordinate based on the palm boundaries, the recognition error caused by a user who slightly rotate or shift his/her hand is minimized. Fig. 4.2 illustrates the procedure of ROI locating:

1. Binarise the input image from Fig. 4.2(a) to Fig. 4.2(b). This is done by first applying a low pass Gaussian smoothing filter on the original image and then apply a threshold T on this result to obtain a binary image.
2. Obtain the boundaries of the gaps, (Fixj, Fiyj) where i = 1,2. This is between the

fingers using a boundary tracking algorithm.

3. Compute the tangent of the two gaps (Fig. 4.2(d)), using this tangent (connect a line passing through (x1,y1) and (x2,y2), any points on (F1xj, F1yj) and (F2xj, F2yj)) is the Y-axis of the palm coordinate;
4. Use a line passing through the midpoint of the two points (x1,y1) and (x2,y2), which is also perpendicular to the Y-axis and call it the X-axis (the line perpendicular to the tangent in Fig. 4.2(d));
5. The ROI is located as a square of fixed size whose center has a fixed distance to the palm coordinate origin (Fig. 4.2(d) and (e));
6. Extract the subimage within the ROI (Fig. 4.2(e) and (f)).

4.3. Palm Vein Extraction by Multi-scale Filtering

From our experience and after analyses, the palm vein widths (cross-sections) in our infrared images varied from 10 pixels to 20 pixels (Fig. 3.7(a)) corresponding to Gaussian with standard derivation from 1.2 to 2.4. In order to produce strong filter responses, the standard derivation of the filters must be similar to the standard derivation of veins. We apply filters (Eq. 3.11) at two different scales 1.8 and 2.6. Notice that 2.6 represents the largest cross-section while 1.8 the smallest. There are two reasons for using larger filter standard derivation: (1) Filters with larger size are

better at denoising and (2) Reorganization will be more tolerance to rotation and shift. Fig. 4.3 shows a single scale filter response. Using either of the two scales will not produce a good response as a lot of noise will be present (Fig. 4.3), hence the need for multi-scale approach.

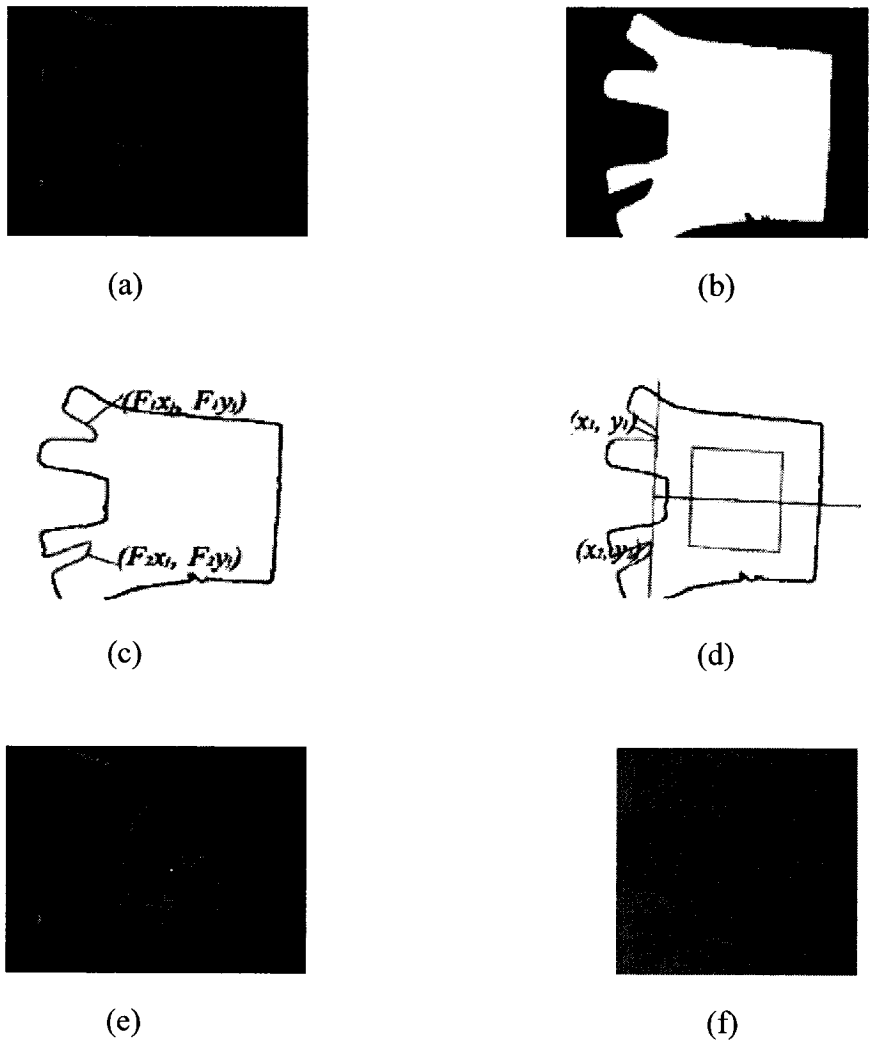

Figure 4.2 ROI location. (a) An infrared palm image captured by our device; (b) Binarized image; (c) Boundaries; (d) and (e) Locating ROI; (f) Subimage of ROI.

(a) (b)

Figure 4.3 (a) Subimage of ROI and (b) the response of its single scale filter.

Fig. 4.4 illustrates the effectives of our multi-scale method giving some examples of thresholding multi-scale products of infrared palm images. Fig. 4.4(a) is a subimage of an infrared palm image within ROI; Fig. 4.4(b) and (c) are filter responses at different scales; Fig. 4.4(d) is the scale production of (b) and (c); Fig. 4.4(e) is the binarised image of (d) and formed using double thresholding (see Section 3.3.2). Finally, Fig. 4.4(f)-(i) are the corresponding images of another palm. The white lines in the binarised images represent palm veins and are used as biometric features in our system. As you can see their width information is retained.

4.4. Matching

Using the palm vein binary image as templates, the similarity of two palms can be calculated by template matching. This is done without any further processing on the binary image and is made possible by the fact that the line widths are well preserved.

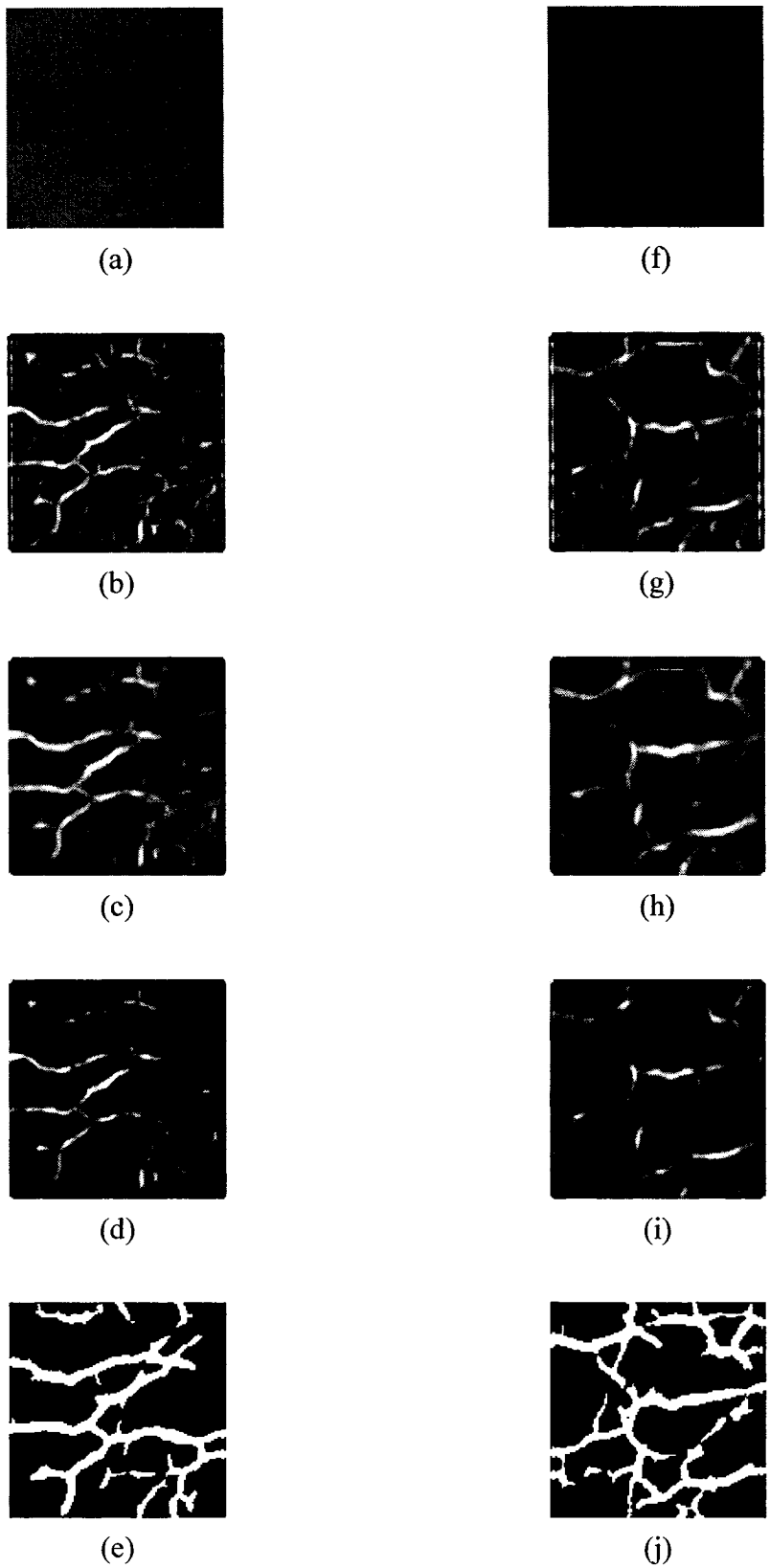

Figure 4.4 Thresholding multi-scale products. (a) A subimage, (b) & (c) Its filter responses at two different scales, (d) Scale production, (e) Binarised image; (f)-(j) Corresponding images of another palm.

Let W denote an existing template in the database and F denote the palm vein image of a new input palm, we match W and F through the logical exclusive or operation. The matching score of W and F are calculated as:

$$S(W,F) = \frac{1}{M \times N} \sum_{i=1}^{M} \sum_{j=1}^{N} \left[\overline{W(i,j) \oplus F(i,j)} \right] \tag{4.1}$$

where $M \times N$ is the size of W or F (W and F must be the same size), $\oplus$ is the logical exclusive or operation and $-$ is the logical "not" operation. The templates W and F taken from the same person are not guaranteed to be the equal. This is because the palm placed inside the capturing device may rotate slightly from one capture to another. To overcome this problem we vertically and horizontally translate the template W a few points and then apply (Eq. 4.1) leading to the final matching score as the maximum matching score of all the translated positions. This matching procedure is illustrated in Fig. 4.5.

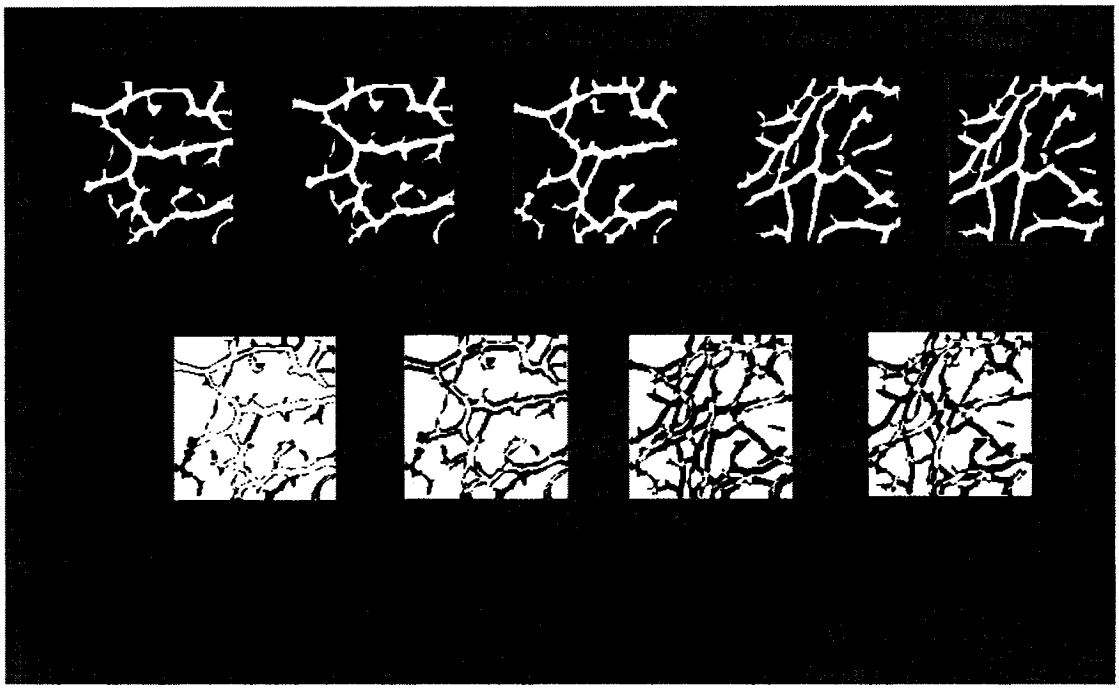

Figure 4.5 Matching procedure.

4.5. Experimental Results

The database we used to test our system consisted of 144 infrared palm images from 24 individuals, each having 6 images. Fig. 4.6 shows images of the palm captured at different times where the image quality is good and Fig. 4.7 shows images of the palm captured at different times where the image quality is bad.

The probability distribution of genuine and imposter is shown in Fig. 4.8. The recognition performance is shown in Fig. 4.9 using ROC curve. We achieved a 98.8% recognition rate where the false acceptance rate was 5.5%. Most of the false recognitions were caused by poor image quality.

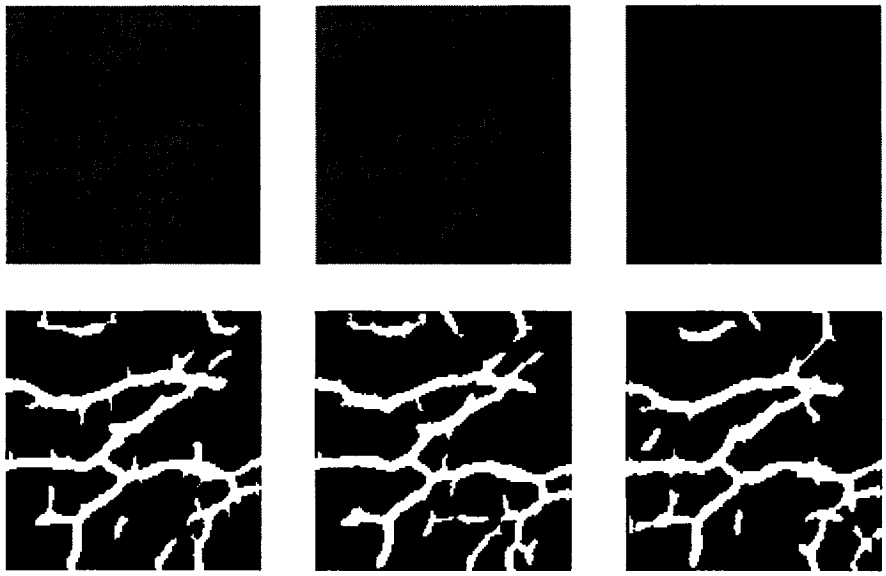

Figure 4.6 Images of a palm captured at different times, where the image quality is good. The first row shows the images captured by our device. The second row shows the corresponding vein extraction results.

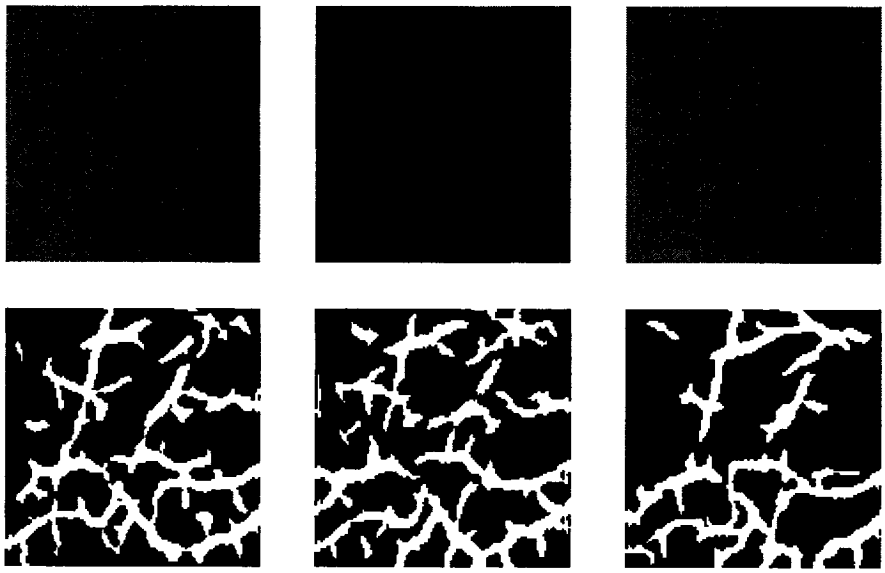

Figure 4.7 Images of a palm captured at different times, where the image quality is bad. The first row shows the images captured by our device. The second row shows the corresponding vein extraction results.

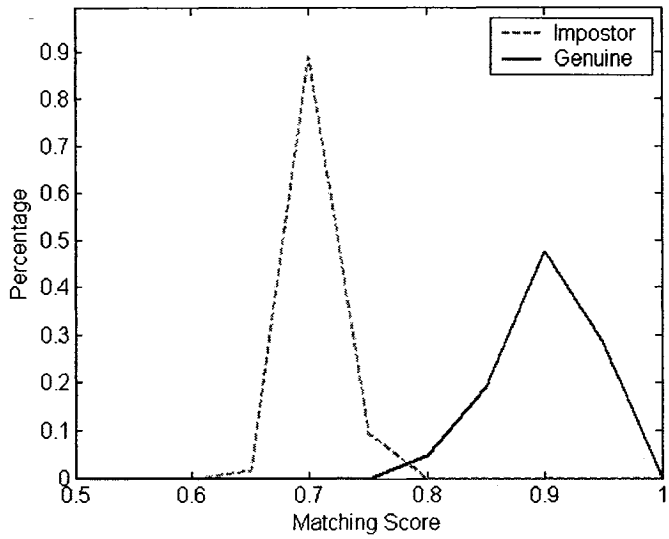

Figure 4.8 The probability distribution of genuine and imposter.

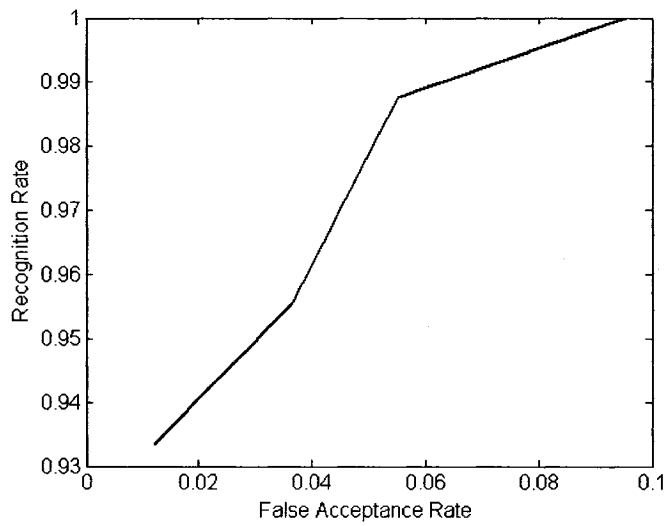

Figure 4.9 System performance evaluation using ROC curve.

Our capture device is very sensitive to outside light. This can affect the infrared light source in such a way that some images have very poor quality, which caused most of the false recognitions. Hence, if the capture device can be improved the system performance will do well. Also, our current database is too small to be convincible and more data is required for a better evaluation of our system.

4.6. Summary

Since palm veins could only be found from a live person, an identification system using this biometrics to detect the liveness of human beings is developed in this chapter. A low cost CCD camera and an infrared light source are used to capture the infrared palm images. A subimage is extracted by locating ROI while the veins within ROI are used as biometric features and extracted using a multi-scale approach. Based on our database, the experimental results demonstrate that the recognition rate of our system is 98.8% where the false acceptance rate is 5.5%.

Chapter 5

Case Study 2:
Retinal Blood Vessel Extraction

This chapter reports our case study of the proposed approach for medical diagnosis applications by retinal blood vessel extractions. Diabetic Retinopathy (DR) is a common complication of diabetes that damages the retina. DR can be classified into four stages: mild Non-Prolifetive Diabetic Retinopathy (NPDR), moderate NPDR, severe NPDR and Prolifetive Diabetic Retinopathy (PDR). If DR is recognized at an early stage treatment can be performed to prevent major vision loss [95]. The appearance of Neovascularization (new vessels growth) stands for PDR [96]. Neovasculars are small, circuit and easy to be tufty. We devise a method for screening DR and help differentiate PDR from NPDR [97]. Section 5.1 explains retinal image capture and preprocessing. The use of multi-scale filtering to detect blood vessels is discussed in Section 5.2. Section 5.3 describes the extraction of retinal vessel patterns and Section 5.4 gives our experimental results. We conclude with a summary of this application in Section 5.5.

5.1. Image Capture and Preprocessing

The color retinal images are first captured using a Kowa VK-2 fundus camera (Fig. 5.1). They are then converted into gray-scale image by modifying the green channel. Some preprocessing operations such as noise reduction by low-pass filter and edge enhancement by histogram equalization are next applied to obtain a clear retinal image with good quality.

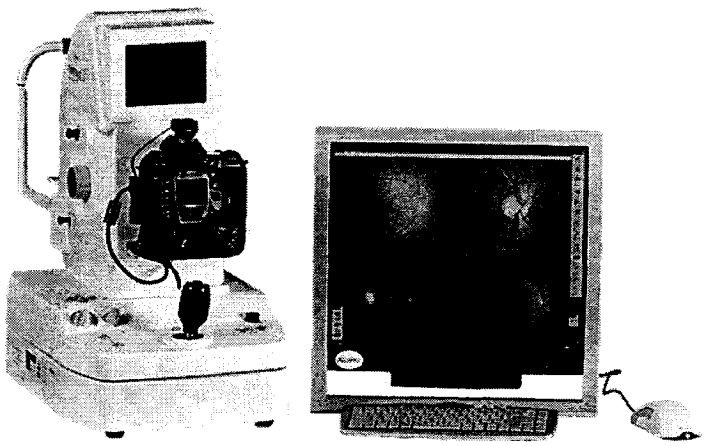

Figure 5.1 Retinal image capture device [98].

5.2. Extracting Blood Vessel by MGF

For PDR detection, most of useful information is located inside small vessels as Neovasculars are petite. For this reason, in order to produce strong filter responses to detect these vessels, σ in the Gaussian Filter (Eq. 3.9) has to be set as small as possible. After examining the cross-sections of retina blood vessels we decided to use

four scales. These scales must be small and be evenly spread out. Using any of these four single Gaussian filters separately will cause more noise in the filter responses. Fig. 5.2 shows this situation. Therefore, to enhance the vessels and suppress noise we use a multi-scale approach.

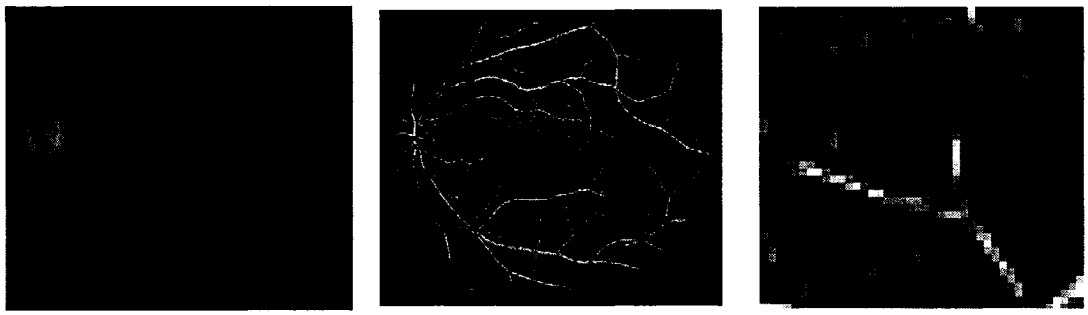

(a) (b) (c)

Figure 5.2 (a) Retinal image, (b) its blood vessels after single scale filter response and (c) cropped and enlarged image of (b).

Fig. 5.3 shows the procedure of our multi-scale vessel extraction approach. The left column shows the vessel extraction for a NPDR image; the right column shows the vessel extraction for a PDR image. Fig. 5.3(a) is a NPDR image; Fig. 5.3(b) and (c) are filter responses (Eq. 3.12) at two different scales (a lot of noise exists in these two images); Fig. 5.3(d) is the scale production (Eq. 3.13) of (b) and (c) (noise is suppressed) and Fig. 5.3(e) is the binarised image of (d) formed using double thresholding (see Section 3.3.2). Fig. 5.3(f)-(j) are the corresponding images of the PDR. From the binary images you can see that the vessel length and width

information are retained. This is important in for the next step.

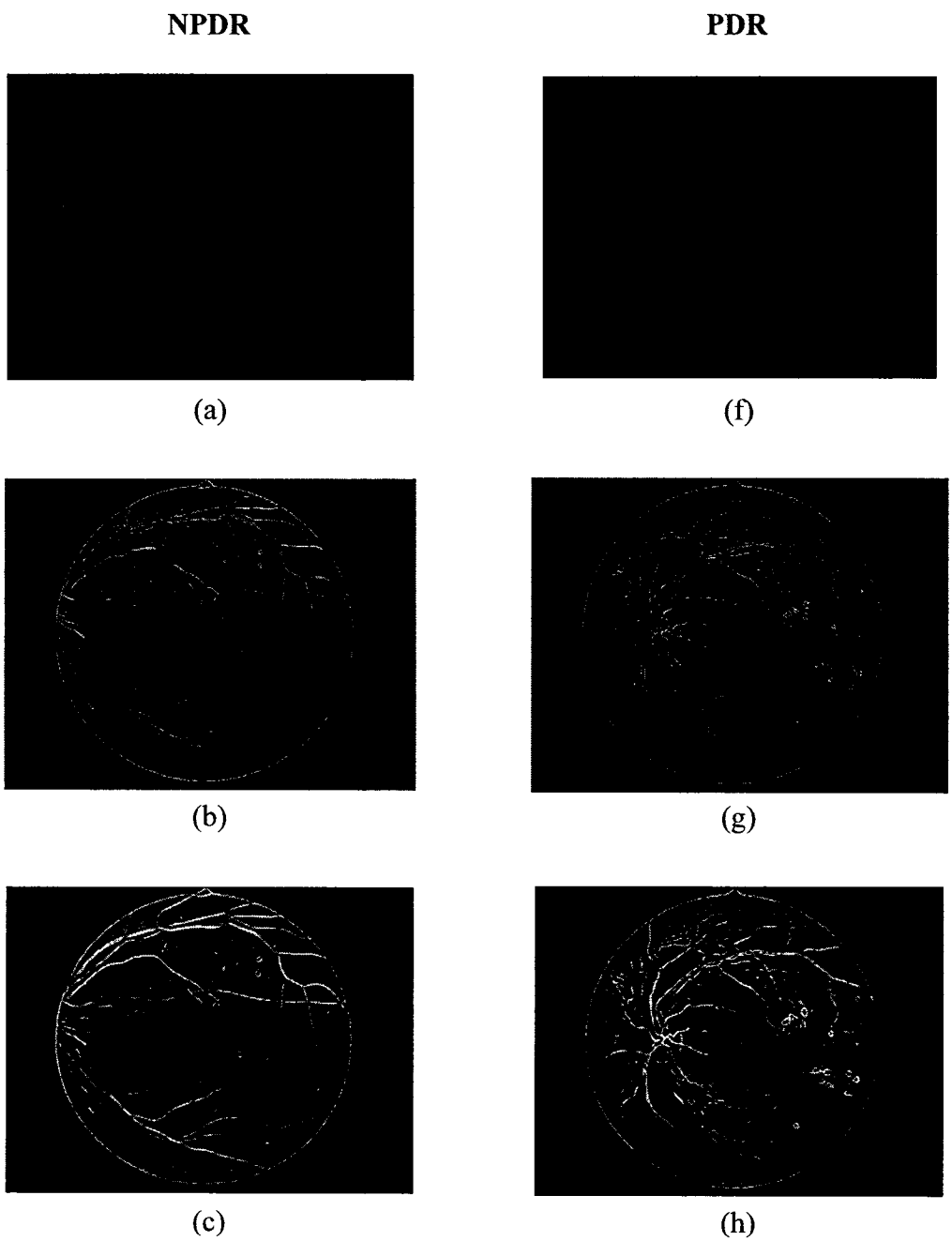

Figure 5.3 Vessel extraction by thresholding multi-scale products.

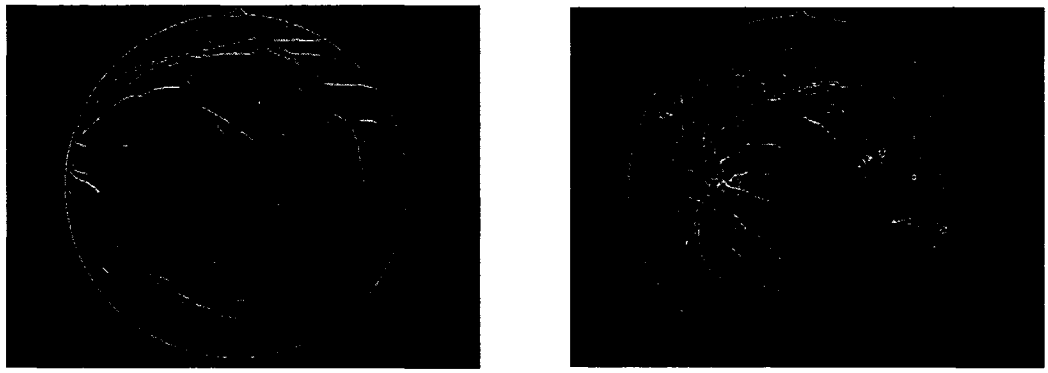

(d) (i)

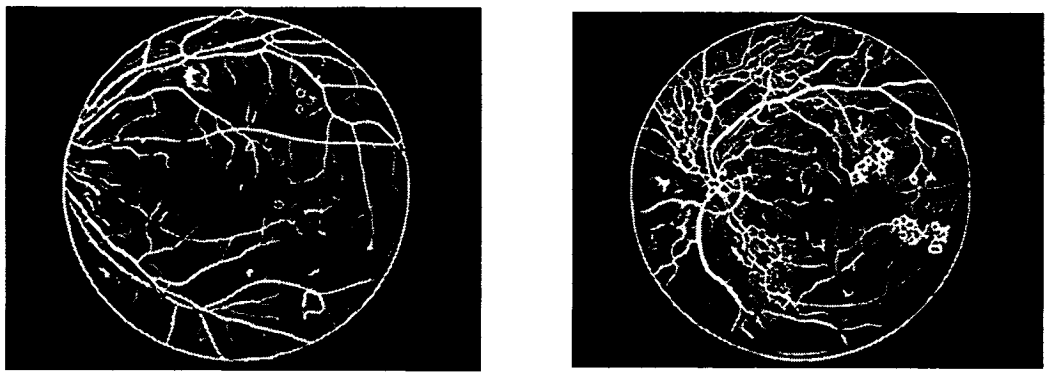

(e) (j)

Figure 5.3 (cont.) Vessel extraction by thresholding multi-scale products.

5.3. Retinal Vessel Patterns

Once the vessels have been enhanced, their patterns can be analyzed through their binarised images (as seen in Fig. 5.3(e) and (j)). As mentioned above, Neovasculars can be defined in Fig. 5.4, which are small, circuit, and easy to be tufty. Circuit means a single vessel changes its direction frequently and tufty means there are more vessels in the retinal region with Neovasculars. We use the term *vessel density* to denote this feature. In Fig. 5.4, there are more cross points of vessels in the retinal region with Neovasculars which resembles a net. We use the term *vessel net density* to denote this

feature. Both vessel density and vessel net density are therefore the features that need to be extracted in a given retinal image. This can be used to distinguish between healthy and ill patients. As an example, two kinds of retinal images are given in Fig. 5.5. We can compare them using both vessel density (shown as a dotted square) and vessel net density (shown as an octagon) features. It is clear that both extracted features (vessel density and vessel net density) in the left image are less compared to the right one.

Figure 5.4 Neovascular representation as the dotted circle.

To analyze both densities, the vessels in Fig. 5.3(e) and Fig. 5.3(j) have to be first thinned to a single pixel width. Fig. 5.6 gives the thinned images of Figs. 5.3(e) and (j). The thinning algorithm used was morphological thinning. This is applied on a binary image and produces an output which is another binary image. The algorithm uses the hit-and-miss transform and can be expressed in terms of it:

$$thin(A,B) = A \; - \; hit\text{-}and\text{-}miss(A,B) \qquad (5.1)$$

where A is the original image, B is the structure element applied to A and − is logical subtraction. The thinning operation functions by applying the origin of the structure element to every pixel in the original image while at the same time comparing it with its surrounding image pixels. If the background (zero) and foreground (one) pixels in the structure element matches exactly with the background and foreground pixels in the original image, then the pixel under the origin (of the structure element) is set to zero (background) otherwise, no change occurs. This process is applied many times until no further changes in the image are made.

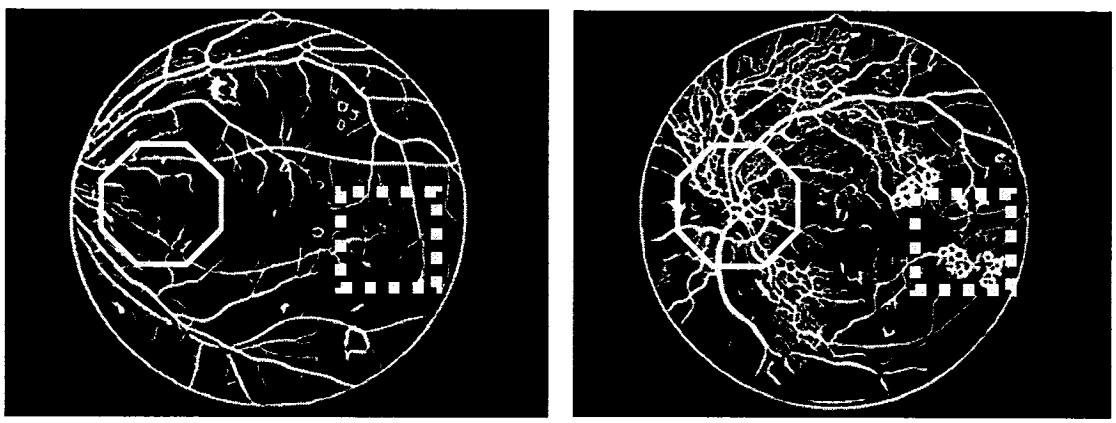

Figure 5.5 Illustration of two kinds of features: Vessel density (dotted square) and Vessel net density (octagon).

As can be seen in Fig. 5.6(b) which is the case of very serious PDR, Neovasculars exists in very small regions (shown in Fig. 5.4) of the retina and

therefore both densities have to be calculated locally. If the size of local window used to calculate the densities is close to the size of the Neovasculars net, the densities should reach their maximum. For each pixel of the thinned image, the vessel points and vessel cross points are counted in its 10*10, 20*20, 50*50 neighborhoods. The maximum of all scales of neighborhoods of all points is regarded as the number of local vessel points and vessel cross points of one image. The vessel density and vessel net density are subsequently calculated by dividing these numbers by the size of the neighborhoods.

5.4. Experimental Results

The database we used was obtained from Ophthalmological Department of the First Affiliated Hospital of Henan Medical College. It contained the color retinal images of 50 patients including 30 NPDR patients and 20 PDR patients. These images were captured using a Kowa VK-2 fundus camera as mentioned before and stored in digital form (with a resolution of 800*608 and 8 bits per color channel).

Fig. 5.7 illustrates the discriminating abilities of vessel density, vessel net density and the fusion of them. Fig. 5.7(a) shows vessel densities of 50 images; Fig. 5.7(b) shows vessel net densities of 50 images; Fig. 5.7(c) shows the fusion of vessel densities and vessel net densities. Because the value range of both vessel density and

vessel net density is between 0-1, the fusion is simply done by calculating their product. Fig. 5.7(a) illustrates that the discriminating ability of vessel density is not good. The discriminating ability of vessel net density (Fig. 5.7(b)) is better than vessel density while the fusion of them (Fig. 5.7(c)) gives the best result.

(a)

(b)

Figure 5.6 (a) Thinned image of Fig. 5.3(e); (b) thinned image of Fig. 5.3(j).

Fig. 5.8 evaluates our system using ROC curve. The True Positive Rate (TPR) is plotted against the False Positive Rate (FPR). TPR means the rate of PDR images being recognized as PDR images. FPR means the rate of NPDR images being

recognized as PDR images. Fig. 5.8 demonstrates that the fusion of vessel density and vessel net density achieves the best performance of TPR 95% at FPR 16.7%. This result shows that screening DR patients and distinguishing PDR from DR through vessel pattern analysis is possible.

The thinning algorithm used is not a good choice as it caused lines to be broken. Most of the false results come from mild PDR. In this case, the vessel density and vessel net density of mild PDR are very similar to NPDR. This means more features are required to distinguish mild PDR from NPDR. The current vessel extraction algorithm should also be improved with the intention to spawn more precise vessel densities.

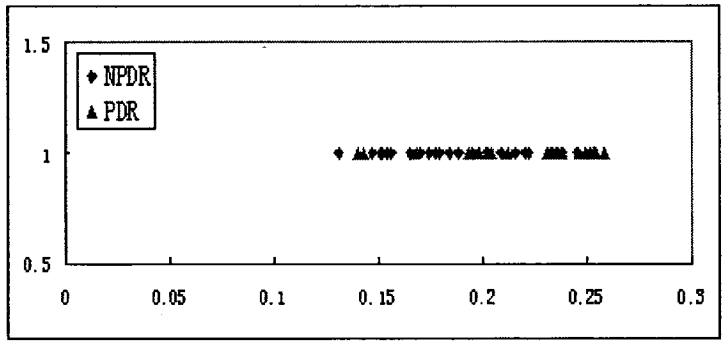

(a)

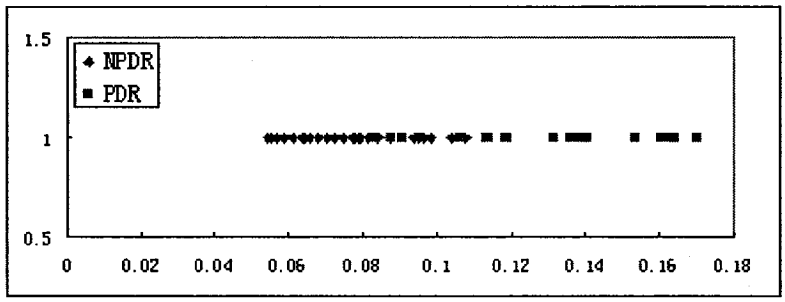

(b)

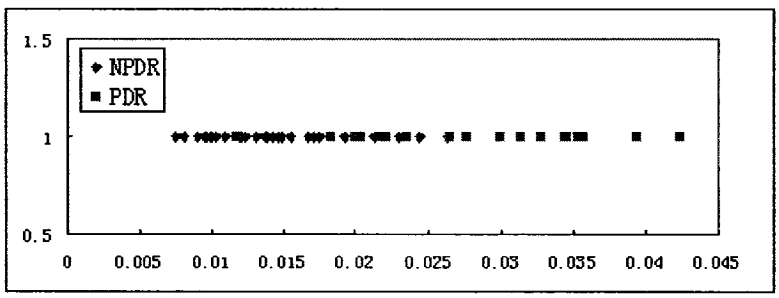

(c)

Figure 5.7 Feature discriminating abilities. (a) Vessel densities of 50 images. (b) Vessel net densities of 50 images. (c) Fusion of vessel densities and vessel net densities.

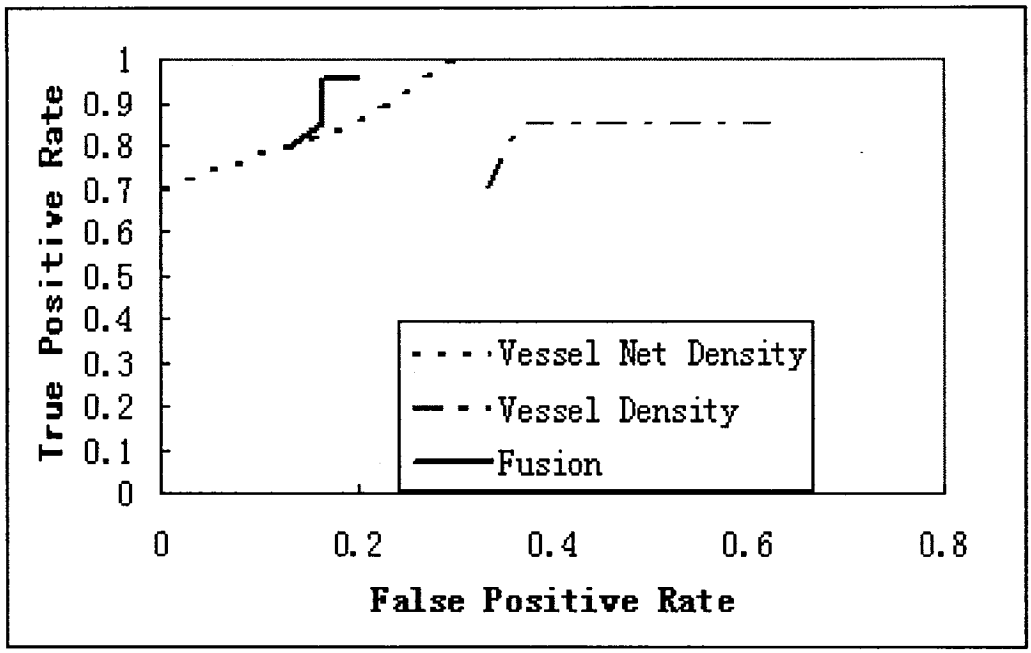

Figure 5.8 System evaluation by ROC curve.

5.5. Summary

Diabetic Retinopathy (DR) is a common complication of diabetes that damages the retina. Recognizing DR as early as possible is very important to protect a patient's vision. We propose a method for screening DR and distinguishing Prolifetive Diabetic Retinopathy (PDR) from Non-Prolifetive Retinopathy (NPDR) automatically through color retinal images. This method evaluates the severity of DR by analyzing the retinal vessel patterns through the features defined as vessel density and vessel net density using a multi-scale approach. The experimental results validate with TPR 95% at FPR 16.7% that the proposed approach can extract wide and thin vessels concurrently. It is also possible to screen DR and distinguish PDR from NPDR using

color retinal images.

Chapter 6

Conclusion and Discussion

This chapter presents the conclusion of our findings of line detection with width information for biometrics systems together with the discussion of the future work.

Along with the automation of our modern life, the need for security has becomes more and more important. Every day questions such as "Should this person be given access to a secure system?", "Does this person have authorization to perform a given transaction?", "Is this person a citizen of our country?" are asked millions of times. All these questions are dealing with the same security issue – how to correctly identify human beings.

Currently there are two popular ways for solving such security problems. One is related to "something that you have", and the other depends on "something that you know". Both methods give the authority to some media such as password or keys and not end users. If a user gets the password or other media he will get the authority otherwise, he will lose the authority. Under such security schema people have to keep various cards and remember tens of passwords. Losing cards or forgetting passwords may cause users great distress. In order to solve this problem researchers are trying various ways and the biometrics approach is most promising. Biometrics is a

technology that uses human being's unique physical or behavioral features to identify or verify persons. Because one's unique characteristics can not be stolen, forgotten, duplicated, shared or observed, biometrics based security system is nearly impossible to fraud.

What biological measurements qualify to be a biometric? Any human physiological and/or behavioral characteristic can be used as a biometric characteristic as long as it satisfies the following requirements: universality, distinctiveness, permanence, collectability, ..., etc.

Various features such as texture, geometry, point and lines exist in the biometric characteristics. One such feature, lines (curvilinear) of different shapes and sizes can be found an array of applications. They are important for the success of higher-level processing such as matching and recognition. Biometric characteristics such as palm veins and retina contain curvilinear features that are the basis used to conduct verification and identification.

In Chapter 2 three traditional methods are presented to detect/extract curvilinear from various applications. They are Hough transform, Differential Geometry and Edge Extraction. Even though these methods can be applied to detect/extract curvilinear structures, they cannot be used in biometric applications as they fail to detect/extract wide information which improves the accuracy of biometric systems.

Two additional methods were presented that extracted lines with wide information but their deficiency also prevented them from being employed in biometrics. Henceforth, we set out to create an approach which detects/extracts wide line information from biometric curvilinear features.

Gaussian filters introduced in Chapter 3 have existed for many years now and are applied in wide range of applications ranging from neural networks to image processing. We used the Gaussian filter after discovering that the cross-sections of given lines resemble a Gaussian shape. Based on this observation, a Gaussian-shaped filter was devised to detect curvilinear features. An advantage of using this type of filter is to preserve the width of the line. It is clear that the wide line information can help to create a more unique template in order to increase the matching accuracy and thus better identify an individual.

We first devise a single scale filter to match the cross-section of the line which produced a response. The idea of single scale did not fair well as there are a lot of noise in this response. To fix this inadequacy, we then turn to multi-scale and scale production where there are three scales and eight directions. The three scales are based on the cross-section of different line widths and the eight directions cover all possible orientations. By combining the individual scale responses using scale production, noise significantly is reduced while preserving important features.

Two case studies are reported and analyzed with experimental details using our proposed approach. One is in the detection of palm veins for identification and liveness discussed in Chapter 4. The other uses retina blood vessels to identify Diabetic Retinopathy (DR) in Chapter 5. The first application uses two scales to preserve the widths of the veins in order to better match the templates (which are binary palm images). For the retina blood vessel application, four small scales are applied in order to match Neovascular. The widths of the vessels are also conserved for the purpose to map out their curvilinear structure. Both applications employing our multi-scale approach produced satisfactory results and demonstrate the importance of wide information.

It should be pointed out that our multi-scale approach can be improved by flexible selection of scales. Our initial experimental results show that scales cannot be randomly selected as this would affect the outcome of the responses. If the scale is too small a lot of noise will persist and if too large, finite details will be lost. Currently there is no definite way of choosing scales. As a part of future work, the approach can be improved to select scales automatically.

In summary, there are many other different biometrics that require wide line information. As part of our future work we will apply the multi-scale approach to other biometric characteristics such as palm-line, knuckle-line and tongue-line

[99-100].

References

[1] G. Roethenbaugh, "Biometrics Explained," Available: *http://www.icsa.net/services/ consortia/cbd-c/sec4.html*

[2] R. Clarke, "Human Identification In Information Systems: Management Challenges And Public Policy Issues," *Info. Technol. People*, vol. 7, no. 4, pp. 6-37, 1994

[3] D. Sims, "Biometrics Recognition: Our Hands, Eyes and Faces Give Us Away," *IEEE Computer Graphics and Applications,* vol. 14, no. 5, pp. 14-15, 1994

[4] J.D. Woodward, "Biometrics: Privacy's Foe or Privacy's Friend?," *Proc. IEEE Special Issue on Automated Biometrics,* vol. 85, no. 9, pp. 1480-1492, 1997

[5] A. Jain, L. Hong, and S. Pankanti, "Biometric identification", Communications of the ACM, vol. 43, no. 2, pp. 90-98, 2000

[6] B. Carter, "Biometrics Technologies, What They Are and How They Work," in *Proc. CTST'97*, 1997

[7] R. Chandrasekaran, "Brave New Whorl: ID System Using The Human Body Are

Here, But Privacy Issues Persist," *Washington Post*, Mar. 30, 1997

[8] A. Davis, "The Body as Password," *Wired*, July 1997.

[9] D.R. Richards, "Rules of Thumb For Biometrics Systems," *Security Manage*, Oct. 1, 1995

[10] G. Lawton, "Biometrics: A New Era in Security," *IEEE Computer*, vol. 31, no. 8, pp. 16-18, 1998

[11] R. Mandelbaum, "Vital Signs of Identity," *IEEE Spectrum*, vol. 31, no. 2, pp. 22-30, 1994

[12] M. Turk and A. Pentland, "Eigenfaces for Recognition," *Journal of Cognitive Neuroscience*, vol. 3, no. 1, pp.71-86, 1991

[13] H.C. Lee and R.E. Gaensslen, editors, *Advances in Fingerprint Technology*, Elsevier, New York, 1991

[14] D. Maio, D. Maltoni, R. Cappelli, J. L. Wayman, and A. K. Jain, "FVC2002: Fingerprint Verification Competition", *Proc. International Conference on Pattern Recognition (ICPR)*, pp. 744-747, Quebec City, Canada, August 2002

[15] V.S. Srinivasan and N.N. Murthy, "Detection of Singular Points in Fingerprint Images", *Pattern Recognition*, vol. 25, no. 2, pp. 139-153, 1992

[16] B.M. Mehtre, "Fingerprint Image Analysis for Automatic Identification," *Machine Vision and Applications*, vol.6, no. 3, pp. 124-139, 1993

[17] R.P. Wildes, "Iris Recognition: An Emerging Biometrics Technology," *Proceedings of the IEEE*, vol.85, no.9, pp. 1348-1363, 1997

[18] Daugman J, "Recognizing Persons by Their Iris Patterns," in: *Biometrics: Personal Identification in Networked Society.* Amsterdam: Kluwer, pp 103-121, 1998

[19] F.H Adler, *Physiology of the Eye: Clinical Application* (fourth edition), The C.V. Mosby Company, London , 1965

[20] J. Rohen, "Morphology and Pathology of the Trabecular Meshwork," in: *The Structure of the Eye*, ed. Smelser, pp. 335-341, Academic Press, New York, 1961

[21] P.W Hallian, "Recognizing Human Eyes," *Geometric Methods Computer Vision*, vol. 1570, no. 9, pp. 214-216, 1991

[22] K. Han and I.K. Sethi, "Handwritten Signature Retrieval and Identification,"

Pattern Recognition Letters, vol. 17, no. 1, pp. 83-90, 1996

[23] R. Plamondon and G. Lorette, "Automatic Signature Verification and Writer Identification – The State of the Art," *Pattern Recognition*, vol. 1, no. 2, pp. 107-131, 1989

[24] D.O. Shaugnessy, "Speaker Recognition," *IEEE ASSP Magazine*, vol. 3, no. 4, pp. 4-17, 1986

[25] W. Shu and D. Zhang, "Automated Personal Identification by Palmprint," *Optical Engineering*, vol. 37, no. 8, pp. 2659-2362, 1998

[26] D. Zhang, W. K. Kong, J. You, M. Wong, "Online Palmprint Identification," *IEEE Trans. on Pattern Analysis and Machine Intelligence*, vol. 25, no. 9, pp. 1041-1050, 2003

[27] W. Shu, G. Rong, Z. Bian, and D. Zhang, "Automatic Palmprint Verification", *International Journal of Image and Graphics*, vol. 1, no. 1, pp. 135-152, 2001

[28] C.C. Han, H.L. Cheng, K.C. Fan, C.L. Lin, "Personal Authentication Using Palmprint Features," *Pattern Recognition*, vol. 36, no. 2, pp. 371-381, 2003

[29] A.K. Jain, A. Ross, and S. Prabhakar, "An Introduction to Biometric

Recognition," *IEEE Trans. Circuits and Systems for Video Technology*, vol. 14, no. 1, pp. 4-20, 2004

[30] M. Golfarelli, D. Maio and D. Maltoni, "On the Error-Reject Trade-Off in Biometrics Verification Systems," *IEEE Trans. Pattern Analysis and Machine Intelligence*, vol. 19, no. 7, pp. 786-796, 1997

[31] W. Shen, M. Surette and R. Khanna, "Evaluation of Automated Biometrics-Based Identification And Verification Systems," *Proc. IEEE Special Issue on Automated Biometrics,* vol. 85, no. 9, pp. 1464-1478, 1997

[32] http://networks.siemens.com/voip/carrier-de/support-nbsp-nbsp-training/pof-1-03-artikel-14-sicherheit-experten-interview.html

[33] http://www.solutionexpert.com.hk/products_services/HandReader_HandPunch.htm

[34] http://pcworld.com/news/

[35] G.J. Awcock and R. Thomas, *Applied Image Processing*, McGraw-Hill, Inc., 1996

[36] D. Behar, J. Cheung, and L. Kurz, "Contrast Techniques for Line Detection in a

Correlated Noise Environment," *IEEE Trans. Image Processing*, vol. 6, no. 5, pp. 625-641, 1997

[37] G.J. Genello, J.F.Y. Cheung, S.H. Billis, and Y. Saito, "Graeco-latin Squares Design for Line Detection in the Presence of Correlated Noise," *IEEE Trans. Image Processing*, vol. 9, no. 4, pp. 609-622, 2000

[38] G.M. Schuster and A.K. Katsaggelos, "Robust Line Detection using a Weighted MSE Estimator," *Proc. Int'l Conf. Image Processing (ICIP'03)*, vol. 1, pp. 293-296, 2003

[39] H. Li, W. Hsu, M.L. Lee and H. Wang, "A Piecewise Gaussian Fodel for Profiling and Differentiating Retinal Vessels," *Proc. Int'l Conf. Image Processing (ICIP'03)*, vol. 1, pp. 1069-1072, 2003

[40] E.R. Davies, M. Bateman, D.R. Mason, J. Chambers and C. Ridgway, "Design of Efficient Line Segment Detectors for Cereal Grain Inspection," *Pattern Recognition Letters*, vol. 24, pp. 413-428, 2003

[41] Z.Y. Liu, K.C. Chiu and L. Xu, "Strip Line Detection and Thinning by RPCL-Based Local PCA," *Pattern Recognition Letters*, vol. 24, no. 14, pp. 2335-2344, 2003

[42] C. Steger, "An Unbiased Detector of Curvilinear Structures," *IEEE Trans. Pattern Anal. Machine Intell.*, vol. 20, no. 2, pp. 113-125, 1998

[43] R. Zwiggelaar, S.M. Astley, C.R.M. Boggis, and C.J. Taylor, "Linear Structures in Mammographic Images: Detection and Classification," I*EEE Trans. Medical Imaging*, vol. 23, no. 9, pp. 1077-1086, 2004

[44] C. Coppini, M. Demi, R. Poli, and G. Valli, "An Artificial Vision System for X-ray Images of Human Coronary Trees," *IEEE Trans. Pattern Anal. Machine Intell.*, vol. 15, no. 2, pp. 156-162, 1993

[45] A. Hoover, V. Kouznetsova, and M. Goldbaum, "Locating Blood Vessels in Retinal Images by Piecewise Threshold Probing of a Matched Filter Response," *IEEE Trans.Med. Imag.*, vol. 19, no. 3, pp. 203-210, 2000

[46] J.B.A. Maintz, P.A. van den Elsen, and M.A. Viergever, "Evaluation of Ridge Seeking Operators for Multimodality Medical Image Matching," *IEEE Trans. Pattern Anal. Machine Intell.*, vol. 18, no. 4, pp. 353-365, 1996

[47] B. Pang and D. Zhang, "Computerized Tongue Diagnosis Based on Bayesian Networks," *IEEE Trans. on Biomedical Engineering*, vol. 51, no. 10, pp. 1803-1810, 2004

[48] S. Mori and T. Sakakura, "Line Filtering and its Application to Stroke Segmentation of Handprinted Chinese Characters," *Proc. Int'l Conf. Pattern Recognition*, vol. 24, no. 1, pp. 366-369, 1984

[49] L.H. Chen, J.Y. Wang, H.Y. Liao, and K.C. Fan, "A Robust Algorithm for Separation of Chinese Characters from Line Drawings," *Image and Vision Computing*, vol. 14, no. 10, pp. 753-761, 1996

[50] C.J. Taylor and D.J. Kriegman, "Structure and Motion from Line Segments in Multiple Images," *IEEE Trans. Pattern Anal. Machine Intell.*, vol. 17, no. 11, pp. 1021-1032, 1995

[51] Z.Y. Zhang, "Estimating Motion and Structure from Correspondences of Line Segments between Two Perspective Images," *IEEE Trans. Pattern Anal. Machine Intell.*, vol. 17, no. 12, pp. 1129-1139, 1995

[52] L. Zhang and D. Zhang, "Characterization of Palmprints by Wavelet Signatures via Directional Context Modeling," *IEEE Trans. SMC-B*, vol. 34, no. 3, pp. 1335-1347, 2004

[53] R.O. Duda and P.E. Hart, "Use of the Hough Transformation to Detect Lines and Curves in Pictures," *Comm. ACM*, vol. 15, no. 1, pp. 11-15, 1972

[54] J. Illingworth and J. Kittler, "A Survey of the Hough Transform," *Computer Vision, Graphics, and Image Processing*, vol. 44, pp. 87–116, 1988

[55] V.F. Leavers, "Which Hough Transform?" *CVGIP: Image Understanding*, vol. 58, no. 2, pp. 250–264, 1993

[56] http://rkb.home.cern.ch/rkb/AN16pp/img459.gif

[57] D.H. Ballard, "Generalizing the Hough Transform to Detect Arbitrary Shapes," *Pattern Recognition*, vol. 13, no. 2, pp. 111–122, 1981

[58] R.M. Haralick, "Ridges and Valleys on Digital Images," *Comput. Vision, Graphics, Image Processing*, vol. 22, pp. 28-38, 1983

[59] J.B. Subirana-Vilanova and K.K. Sung, "Ridge-Detection for the Perceptual Organization without Edges," *the 4th Int'l Conf. Computer Vision*, pp. 57-64, Berlin, Germany, 1993

[60] L.A. Iverson and S.W. Zucker, "Logical/Linear Operators for Image Curves," *IEEE. Trans. Pattern Analysis and Machine Intelligence*, vol. 17, no. 10, pp. 982-996, 1995

[61] A. Busch, "Revision of Built-up Areas in a GIS using Satellite Imagery and GIS

Data," *Proceedings of IAPRS*, vol. 32, part 4, pp. 91-98, 1998

[62] T. Linderberg, "Edge Detection and Ridge Detection with Automatic Scale Selection," *Int'l J. Computer Vision*, vol. 30, no. 2, pp. 117-154, 1998

[63] M. Jacob and M. Unser, "Design of Steerable Filters for Feature Detection using Canny-like Criteria," *IEEE Trans. Pattern Anal. Machine Intell.*, vol. 26, no. 8, pp. 1007-1019, 2004

[64] D. Eberly, R. Gardner, B. Morse, S. Pizer, and D. Scharlah, "Ridges for Image Analysis," *J. Math. Imaging and Vision*, vol. 4, no. 4, pp. 353-373, 1994

[65] A. Busch, "A Common Framework for the Extraction of Lines and Edges," *Int'l Archives of Photogrammetry and Remote Sensing*, vol. 31, part B3, pp. 88-91, 1996

[66] D. Geman and B. Jedynak, "An Active Testing Model for Tracking Roads in Satellite Images," *IEEE Trans. Pattern Anal. Machine Intell.*, vol. 18, no. 1, pp. 1-14, 1996

[67] N. Merlet and J. Zerubia, "New Prospects in Line Detection by Dynamic Programming," *IEEE Trans. Pattern Anal. Machine Intell.*, vol. 18, no. 4., pp.

426-431, 1996

[68] J.H. Jang and K.S. Hong, "Detection of Curvilinear Structures using the Euclidean Distance Transform," *Proc. IAPR Workshop on Machine Vision Applications*, pp. 102-105, 1998

[69] A.W.K. Loh, M.C. Robey, and G.A.W. West, "Analysis of the Interaction between Edge and Line Finding Techniques," *Pattern Recognition*, vol. 34, no. 6, pp. 1127-1146, 2001

[70] J.H. Jang and K.S. Hong, "Linear Band Detection based on the Euclidean Distance Transform and a New Line Segment Extraction Method," *Pattern Recognition*, vol. 34, no. 9, pp. 1751-1764, 2001

[71] D.S. Guru, B.H. Shekar, and P. Nagabhushan, "A Simple and Robust Line Detection Algorithm Based on Small Eigenvalue Analysis," *Pattern Recognition Letters*, vol. 25, no. 1, pp. 1-13, 2004

[72] J. Canny, "A Computational Approach to Edge Detection," *IEEE Trans. Pattern Anal. Machine Intell.*, vol. 8, no. 6, pp. 679-698, 1986

[73] Q. Li, Z. Qiu, D. Sun, "Personal Identification Using Knuckleprint,"

Sinobiometric04', *Lecture Notes in Computer Science*, vol. 3338, pp. 680-689 2004

[74] X.Q. Wu, K.Q. Wang, D. Zhang, "Palm-line Extraction and Matching for Personal Authentication," *IEEE Trans. SMC-A* vol. 36 no. 5, pp. 978-987, 2006

[75] J. Chen, Y. Sato, and S. Tamura, "Orientation Space Filtering for Multiple Orientation Line Segmentation," *IEEE Trans. Pattern Anal. Machine Intell.*, vol. 22, no. 5, pp. 417-429, 2000

[76] K. R. Castleman, *Digital Image Processing*. Prentice Hall, Inc., 1996

[77] Wang, L., Leedham, G, "A Thermal Hand Vein Pattern Verification System," *In Pattern Recognition and Image Analysis, Lecture Notes in Computer Science*, vol. 3687, pp. 58-65, 2005

[78] C. L. Lin and K. C. Fan, "Biometric Verification Using Thermal Images of Palm-Dorsa Vein Patterns," *IEEE Transactions On Circuits And Systems For Video Technology*, vol. 14, no. 2, pp. 199-213, 2004

[79] C.Y. Suen and T.Y. Zhang, "A Fast Parallel Algorithm for Thinning Digital Patterns," *Communications of the ACM 27*, vol. 3, pp. 236-239, 1984

[80] Huiqi Li, Opas Chutatape, "Automated Feature Extraction in Color Retinal Images by a Model based Approach," *IEEE Transactions on Biomedical Engineering*, vol. 51, no. 2, pp. 246-254, 2004

[81] T. Chanwimaluang and G. Fan, "An Efficient Algorithm for Extraction of Anatomical Structures in Retinal Images," *IEEE International Conference on Image Processing*, vol. 1, pp. 1093-1096, 2003

[82] A. Can, H. Shen, J. N. Turner, H. L. Tanenbaum, and B. Roysam, "Rapid Automated Tracing and Feature Extraction from Retinal Fundus Images using Direct Exploratory Algorithms," *IEEE Trans.Inf.Technol. Biomed.*, vol. 3, no. 2, pp. 125-138, 1999

[83] L. Gang, O. Chutatape, and S. Krishnan, "Detection and Measurement of Retinal Vessels in Fundus Images using Amplitude Modified Second-Order Gaussian Filter," *IEEE Trans.Biomed. Eng.*, vol. 49, no. 2, pp. 168-172, 2002

[84] S. Chaudhuri, S. Chatterjee, N. Katz, M. Nelson, and M. Goldbaum, "Detection of Blood Vessels in Retinal Images using Two-dimensional Matched Filters," *IEEE Trans. on Medical Imaging*, vol. 8, no. 2, pp. 263–269, 1989

[85] T.M. Koller, G. Gerig, G. Szekely, and D. Dettwiler, "Multiscale Detection of

Curvilinear Structures in 2-D and 3-D Image Data," *the 5th Int'l Conf. Computer Vision*, pp. 864-869, Boston, USA, 1995

[86] http://cnx.org/content/m13859/latest/SignalNoise.png

[87] J.C. Russ, *The Image Processing Handbook*, CRC Press, 1999

[88] http://www-mmdb.iai.uni-bonn.de/lehre/BIT/ss03_DSP_Vorlesung/matlab_demos/images/filters/gaussian_convolution_filter/filter_5.0.JPG

[89] S. Mallat and S. Zhong, "Characterization of Signals From Multiscale Edges," *IEEE Trans. Pattern Analysis and Machine Intelligence*, vol. 14, no. 7, pp. 710–732, 1992

[90] P. Bao and L. Zhang, "Noise Reduction for Magnetic Resonance Image via Adaptive Multiscale Products Thresholding," *IEEE Trans. on Medical Imaging*, vol. 22, no. 9, pp. 1089-1099, 2003

[91] P. Bao, L. Zhang, and X. L. Wu, "Canny Edge Detection Enhancement by Scale Multiplication", *IEEE Trans. Pattern Analysis and Machine Intelligence*, vol. 27, no. 9, 2005

[92] Q. Li, J. You, L. Zhang, D. Zhang, and P. Bhattacharya, "A New Approach to

Automated Retinal Vessel Segmentation Using Multiscale Analysis," *IEEE ICPR*, vol. 4, pp. 77-80, 2006

[93] J. V. B. Soares, J. J. G. Leandro, R. M. Cesar Jr., H. F. Jelinek, and M. J. Cree, "Retinal Vessel Segmentation Using the 2-D Gabor Wavelet and Supervised Classification," *IEEE Trans. Med. Imag.*, vol. 25, no. 9, pp. 1214–1222, 2006.

[94] Y. Zhang, Q. Li, J. You, and P. Bhattacharya, "Palm Vein Extraction and Matching for Personal Authentication," *9th International Conference on Visual Information Systems*, 2007

[95] H. R. Taylor and J. E. Keeffe, "World Blindness: A 21st Century Perspective," *Brit. J. Ophthalmol.*, vol. 85, pp. 261–266, 2001

[96] 5. E. J. Sussman, W. G. Tsiaras, and K. A. Soper, "Diagnosis of Diabetic Eye Disease," *J. Am. Med. Assoc.*, vol. 247, pp. 3231–3234, 1982

[97] Q. Li, Y. Zhang, X. Jin, J. You, and P. Bhattacharya, "Screening Prolifetive Diabetic Retinopathy Through Color Retinal Images," *International Conference on Image Processing, Computer Vision, and Pattern Recognition*, 2007

[98] http://www.kowa-usa.com/images/product/Non_Myd_7_System.jpg

[99] B. Pham and Y. Cai, "Visualization Techniques for Tongue Analysis in Traditional Chinese Medicine," *Proc. SPIE*, vol. 5367, pp. 171-180, 2004

[100] D. Zhang, Z. Liu, J. Yan and P. Shi, "Tongue-Print: A Novel Biometrics Pattern," *2nd International Conference on Biometrics*, 27-29 August, Korea University, Seoul, Korea, 2007.

[101] http://biometrics.cse.msu.edu/hand_geometry.html